VOL. 77/DEC. 1996

MITSUBISHI ELECTRIC ADVANCE

1,000kV Power Systems Edition

MITSUBISHI ELECTRIC

A Quarterly Survey of New Products, Systems, and Technology

●Vol. 77/Dec. 1996 Mitsubishi Electric **ADVANCE**

1,000kV Power Systems Edition

CONTENTS

Our cover shows 1,000kV substation equipment undergoing evaluation at Tokyo Electric Power Company's UHV test field. Mitsubishi Electric is responsible for the central phase (except for bushings).

Editorial Inquiries

Masaaki Udagawa
Planning and Administration Dept.
Corporate Engineering, Manufacturing & Information Systems
Mitsubishi Electric Corporation
2-3-3 Marunouchi
Chiyoda-ku, Tokyo 100, Japan
Fax 03-3218-2465

Product Inquiries

Tsuyoshi Uesugi
Strategic Marketing Dept.
Global Operations Group
Mitsubishi Electric Corporation
2-2-3 Marunouchi
Chiyoda-ku, Tokyo 100, Japan
Fax 03-3218-3597

Orders:
Four issues: ¥6,000
(postage and tax not included)
Ohm-sha Co., Ltd.
1 Kanda Nishiki-cho 3-chome
Chiyoda-ku, Tokyo 101, Japan

Mitsubishi Electric Advance is published quarterly (in March, June, September, and December) by Mitsubishi Electric Corporation.

Surge Arrestor Technology for 1,000kV Lines

*by Yoshibumi Yamagata, Mikio Mochizuki and Shinji Ishibe**

High-performance 1,000kV arrestors are indispensable components in the coordination of insulation for 1,000kV power transmission systems. During the development evolution toward 1,000kV arrestors over the past 20 years, drastic improvements have been made in surge arrestor technology. This article describes Mitsubishi Electric's development of a high-performance zinc-oxide element and the 1,000kV arrestor in which the element is incorporated.

Background

With increasing urban power demand and the trend to locate new power plants in remote areas, Japan's power network is growing larger and higher transmission voltages are being used. Introduction of 1,000kV power transmission technology is a key to providing a stable long-term power supply to meet this demand. The testing of substation equipment for 1,000kV power systems began during 1995 at the Shin-Haruna Substation UHV test yard of Tokyo Electric Power Company.

Full-scale development of this substation equipment began in 1990, but R&D on zinc-oxide (ZnO)elements suitable for 1,000kV surge arrestors has been underway since the late 1970s. Economic considerations require that the insulation margins of 1,000kV equipment be reduced dramatically as compared to 500kV equipment, and this must be accomplished without sacrificing reliability. Fig. 1 shows the arrestor protective level required to support the 1,000kV insulation design.

Development of Zinc-Oxide Elements

The elements that comprise a surge arrestor consist of high-purity ZnO mixed with trace amounts of other metallic oxides which are formed and baked at temperatures upwards of 1,000°C. Fig. 2 shows the production process. These elements have useful nonlinear voltage-current characteristics, and can be stacked to provided the desired operating characteristics.

As far back as 1978, the Central Research Institute of the Electric Power Industry, Meidensha Corporation and Mitsubishi Electric tested the switching surge absorption performance of a 1/59 scale model of a 1,000kV surge arrestor. The arrestor was designed using state-of-the-art technology at the time, but the protection level (i.e., residual voltage at a current of 10kV) was still 20~30% higher than actually required. The UHV transmission working group decided that test voltages for 1,000kV equipment should be lower than would be suggested by simply scaling up 500kV equipment. Targets for three levels of protection, A, B and C, were established. Level C, shown in Fig. 1, is the most demanding level and the level to which the 1,000kV arrestors reported here were designed. Level A is 20% higher and level B 10% higher.

In simplest terms, the protection level can be lowered by reducing the number of ZnO elements per stack, but this shortens the element life due to the increased electrical stress. With

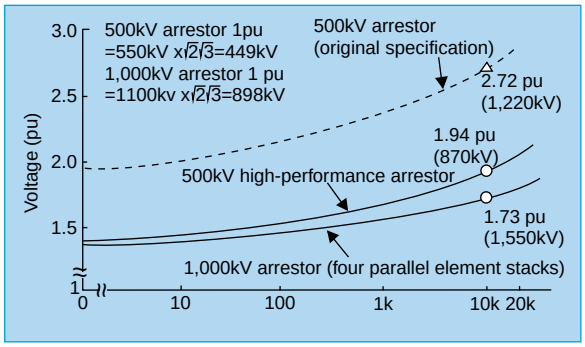

Fig. 1 Surge arrestor voltage-current characteristics.

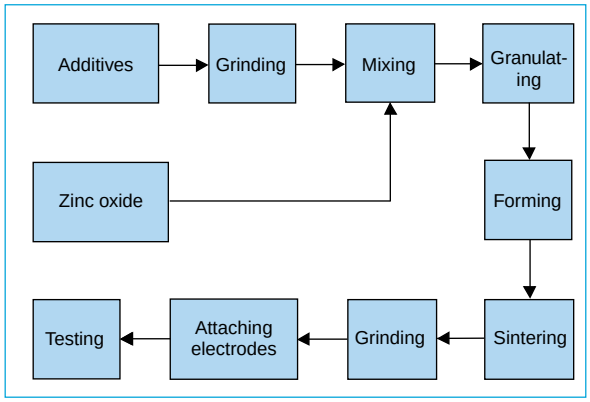

Fig. 2 The ZnO element production process.

Yoshibumi Yamagata is with Tokyo Electric Power Company and Mikio Mochizuki and Shinji Ishibe are with the Itami Works.

Table 1 Specifications of Original and High-Performance 500kV Arrestors

Category		Original	High-performance	1,000kV specifications
General	Type	SF6 gas-insulated tank enclosure	SF6 gas-insulated tank enclosure	SF6 gas-insulated tank enclosure
	Model	MAH-TA	MAU-TA	MAU-TA
	Rated voltage	420kV	420kV	826kV
	Continuous operating voltage	550/√3kV rms	550/√3kV rms	1,100/√3kV rms
	Nominal discharge current	10kA	10kA	20kA
	Lightning impulse withstand voltage	1,550kV	1,425kV	2,250kV
Protection performance	V10kA	1,110kV or less	870kV or less	1,550kV or less
	V20kA	—	—	1,620kV or less
Energy duty	Switching surge	JEC-217 surge (78μF capacitance, corresponding to a 200km transmission line)	JEC-217 surge (78μF capacitance, corresponding to a 200km transmission line)	Switching surge on 221μF capacitance (corresponding to a 250km transmission line)
Other	Temporary overvoltage	>7MJ (1.5 pu for 2s)	>7MJ (1.5 pu for 0.2s)	>55MJ (1.5 pu x 0.55s)
	Dimensions (mm)	1,100 dia. x 3,300	1,018 dia. x 2,580	1,774 x 4,800
	Weight (tons)	4.0	3.5	13
	Relative volume	1.0	0.67	2.35

the manufacturing technologies available in 1978, an element life of 1 ~ 2 years was considered acceptable. Lower protection levels also require arrestors to absorb the energy of switching surges associated with circuit breaker activity and power-frequency temporary overvoltage (TOV) associated with ground faults and load disconnection. These surges cause large arrestor currents and energy at lower protection levels.

By 1982, we had improved the ZnO element characteristics enough to satisfy C-level protection requirements. These improvements took place in three areas.

First, the element life was extended to a long, stable operating life under voltage stress 10 ~ 15% higher than previously possible. This was achieved by incorporating glass-phase components that stabilize the particle boundary layers.

Second, the energy capability per element was extended 40 ~ 50% through changes in the particle-forming process that resulted in more uniform element structure and current flow.

Third, 10% flatter voltage-current characteristics were obtained by lowering the limiting voltage that appears across the element contacts at currents in the range of 5 ~ 20kA. Trivalent metal oxides such as Al_2O_3 were added to improve electron mobility under high-current conditions, the ZnO particle size was reduced and sintering processes were optimized to increase the potential barrier at the grain boundaries.

The arrestor elements we developed for 1,000kV use immediately found applications in lower-voltage power systems. Beginning in 1984, Mitsubishi Electric worked with Tokyo Electric Power Company to improve the protection level of 500kV arrestors. We developed a high-performance arrestor with a 30% lower protection level (Fig. 1) and the same element voltage stress and energy duty as the planned 1,000kV arrestors. This allowed test voltages to be lowered without sacrificing reliability, which led to equipment size and cost reductions and paved the way for the development of 1,000kV arrestors. Table 1 lists the specifica-

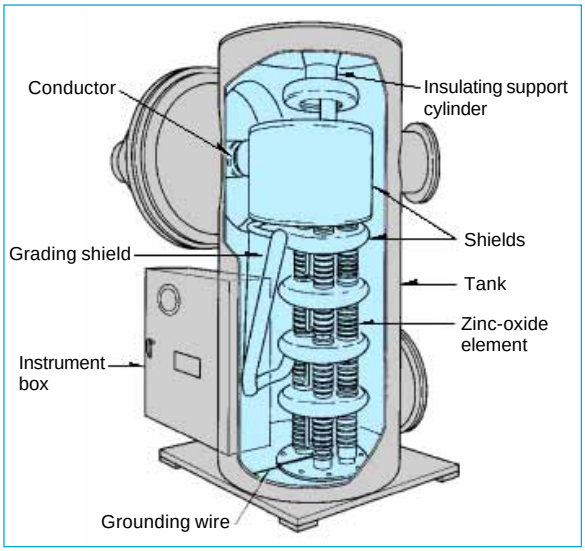

Fig. 3 Construction of a 500kV high-performance arrestor.

tions of the high-performance 500kV arrestors and Fig. 3 shows their construction.

1,000kV Arrestor Development

The 1,000kV arrestor needed to be double the capability of the 500kV arrestor with a 12% reduction in protection level. We achieved this using elements equivalent to two 500kV arrestors arranged in four parallel stacks. Table 1 lists the specifications, Fig. 4 shows the construction and Fig. 5 shows a photograph. The elements are organized as two 500kV units, each consisting of ten 42kV sections stacked in series. Each section consists of four parallel 15-element stacks.

An analysis of the 1,000kV power system led to a TOV energy duty specification of 55MJ. Fig. 6 shows the relationship between transmission voltage and surge arrestor energy duty. The switching surge energy duty requirement is equal to or less than that on the high-performance 500kV arrestors, however, the TOV energy duty is more than double that of the 500kV arrestors. Since this severe duty is nearly at the limit of the element energy capability, a major point for developing 1,000kV arrestors was to achieve an adequate margin for TOV duty. Two innovations not found in 500kV-and-lower voltage arrestors made this possible.

First, the element arrangement was optimized to ensure a more uniform distribution of TOV duty. Because of the nonlinear voltage-current characteristics of the arrestor elements, any differences in the limiting voltage between the four parallel stacks would lead to a concentration of current in the stack with the lowest limiting voltage and therefore nonuniform energy duty. We eliminated these differences by measuring the limiting voltage of each element and selecting elements to create four stacks of nearly identical limiting voltage. The voltage measurement used is the drop across the element while sustaining a current of 100A, which corresponds to 400A through the complete arrestor.

To verify that this method would yield a uniform current distribution, we tested a 42kV section like the one shown in Fig. 4 and measured the current through each stack. Table 2 shows the results. A maximum current variation of 0.5% was measured in stacks adjusted for identical limiting voltages (case 1). A maximum current variation of 4.3% was measured in stacks with 0.08% variation in limiting voltage (case 2). The measured values were close to the numerical predictions of 0% for case 1 and 2.7% for case 2. These results led us to specify 0.15% variation for the 100A limiting voltage,

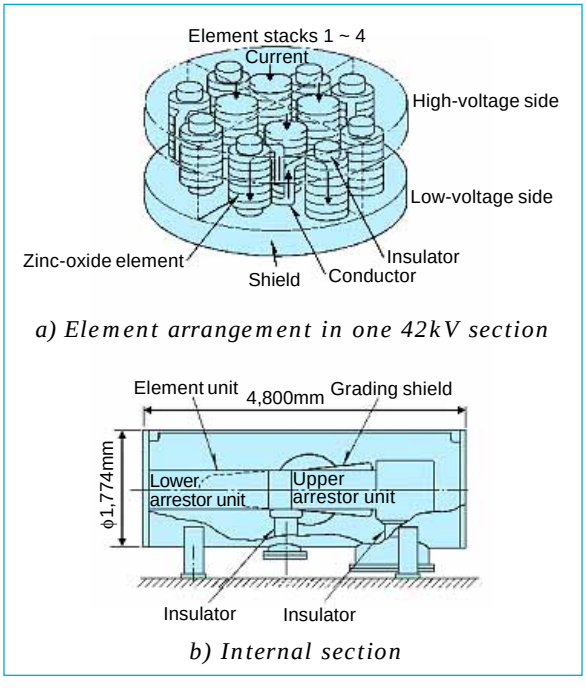

Fig. 4 Construction of the 1,000kV arrestor.

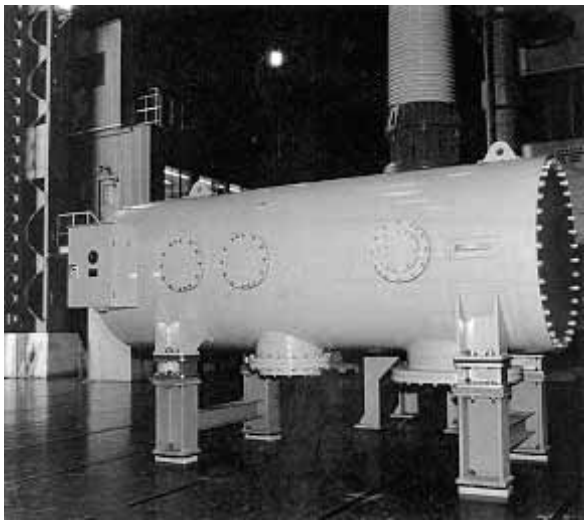

Fig. 5 1,000kV arrestor.

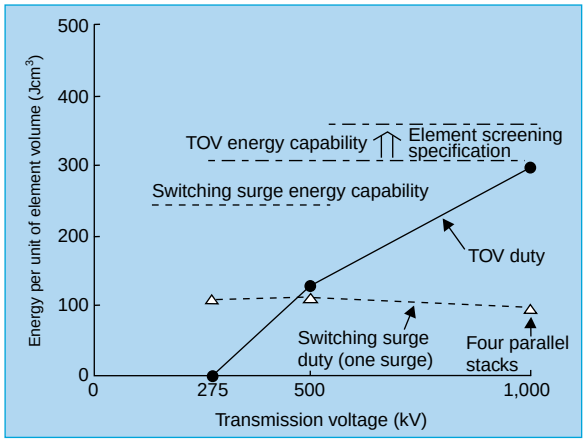

Fig. 6 Surge arrestor energy capability as a function of transmission voltage.

Table 2 Current Uniformity Test Results

	Current waveform	Peak current (A)	Peak current per stack (A)				Variation (%)
			No. 1	No. 2	No. 3	No. 4	
Case 1(0% predicted variation)	8/20μs	498 900 1,648	125 226 412	124 224 414	125 226 412	124 224 410	0.4 0.4 0.5
Case 2 (2.7% predicted variation)	8/20μs	361 1,002 4,992 9,860	89 248 1,232 2,440	88 248 1,240 2,440	94 258 1,272 2,500	90 248 1,248 2,480	4.2 3.0 1.9 1.4
	30/80μs	119 487 978 3,028	29 120 240 744	29 120 242 752	31 126 254 780	30 121 242 752	4.2 3.5 3.9 3.0
	AC	189 441 728 867	46 108 179 213	47 109 181 216	49 115 189 225	47 109 179 213	3.7 4.3 3.8 3.8

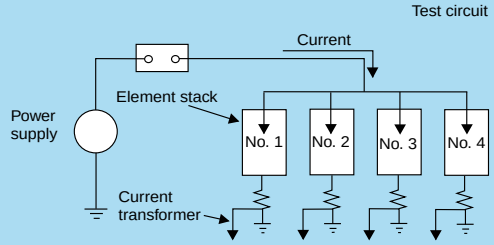

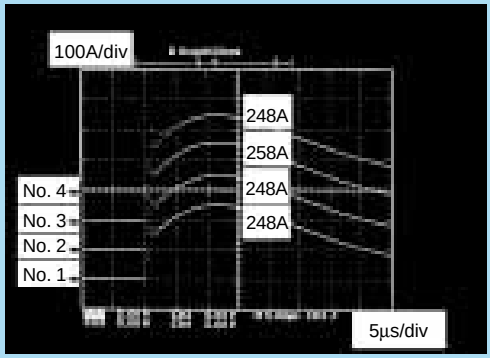

Typical oscilloscope traces for 8/20μs current waveform testing with 1,002A peak current

which computes to 5% variation in current, and to specify the TOV capacity of the completed arrestor assuming 10% current variation.

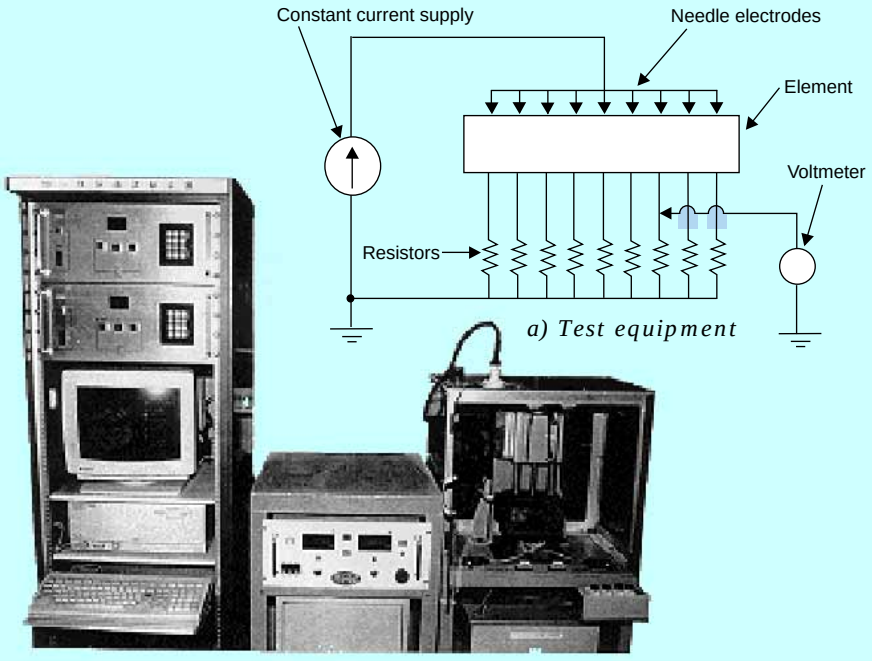

a) Test equipment

b) Test circuit

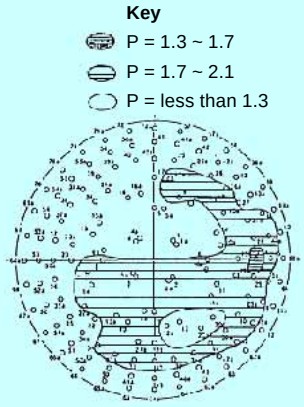

c) Typical current ratio map

Fig. 7 Current uniformity testing of ZnO elements.

Next, elements were screened based on uniformity testing. The chief cause of element destruction during TOV duty is the thermal stress associated with power dissipation. Non-uniform current flow within an element will cause heat concentrations that can lead to element destruction at lower-than-expected energy duty. We therefore tested each element and discarded those exhibiting poor current uniformity. The elements were screened just prior to electrode mounting. A 20mA current was applied to each element through 100 needle-like electrodes and the current through each was measured to give a picture of the current flow uniformity. Fig. 7 shows the testing unit, test circuit and typical current distribution.

We also investigated the relationship between current flow uniformity and energy capability. We conducted destructive TOV testing, applying TOVs until the test element was destroyed, and calculated the energy dissipation. Fig. 8 shows typical test data. Note that the selection of elements was deliberately chosen to provide a wide range of Pmax values. The largest Pmax values occur in specially selected elements.

To screen the elements, we arrived at a uniformity index for each device by dividing the current at each measurement point by the average current and taking the maximum value.

Fig. 9 shows a Weibull plot of TOV energy-capability results obtained from testing the screened elements. The plot shows that the screened elements have a 15% margin over the 300J/cm^3 capability required for an arrestor with 55MJ energy duty using four parallel stacks with 10% current variation.

The completed 1,000kV arrestors have been qualified following earthquake-resistance testing, transport testing, voltage stress testing, heat cycle testing and other test items.

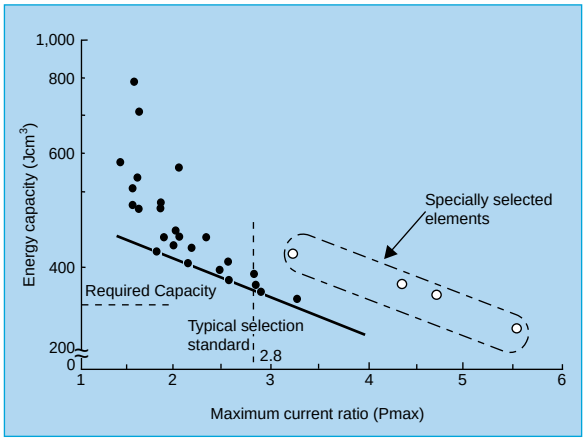

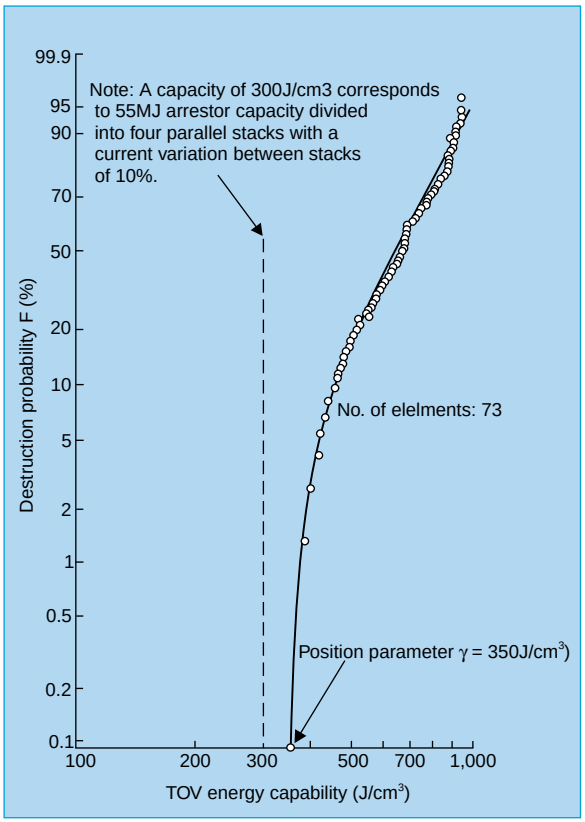

Fig. 9 Weibull plot of element energy capacities.

Mitsubishi Electric has been developing high-performance ZnO element technologies for 1,000kV surge arrestors since the late 1970s. Now that first-generation 1,000kV arrestors are qualified for service, R&D is continuing with the aim of developing smaller arrestors with better performance for more economical and reliable power transmission services. ❑

A 1,000kV Transformer

*by Eiichi Tamaki and Yoshibumi Yamagata**

To provide a stable power supply to meet the increasing electrical demand through the 21st century, Tokyo Electric Power Company (TEPCO) is developing Japan's first 1,000kV transmission systems, and is currently testing the performance, reliability, operation and maintenance of 1,000kV equipment in a 1,000kV test field at its Shin-Haruna Substation. Mitsubishi Electric has been developing a variety of 1,000kV substation equipment, and the Ako Works produced a single-phase 1,000kV shell-form transformer for qualification testing. This article reports on the specifications, construction, installation and testing of the 1,000kV transformer.

Specifications

Table 1 lists the basic transformer specifications. The 1,000kV transformer is a single-phase, autotransformer with an on-load voltage regulator (LVR) at the central point. Extensive studies led to selection of the following specifications.

The primary and secondary bank capacities of 3,000MVA were selected to satisfy maximum transmission capacity. The tertiary capacity of 1,200MVA (40% of the primary and secondary capacities) was selected as the maximum capacity to supply the apparent power required by the 1,000kV transmission lines.

As a tertiary voltage rating of 63kV—the same as 500kV transformers—would result in an excessively large current in a fault condition, a 147kV rating was selected so that the size of the equipment connected to the tertiary winding would not have to be increased.

An impedance value of 18% was chosen in consideration of maximum grid stability, suppression of ground fault currents and economy of transformer design.

Since 1,000kV substations will be constructed in mountainous areas, all transformer components will have to be transportable by rail and oversized tractor-trailer. The main body of the 1,000kV transformer was divided into two units to satisfy the transport limitations.

Two LVRs are provided, one for each unit.

A long-term AC withstand test voltage was selected from a transient overvoltage analysis of the fault conditions of future 1,000kV transmission systems:

$$1.5E\ (1h) \sim \sqrt{3}E\ (5\ min) \sim 1.5E(1h)$$

where $E = 1{,}100/\sqrt{3}$kV, without partial discharge during testing.

The lightning impulse withstand test voltage was determined by analyzing the transient voltage levels in 1,000kV systems with high-performance lightning arrestors; 1,950kV primary and 1,300kV secondary withstand voltages were selected.

A noise level of 65 dB was specified to minimize the environmental noise of the substation. This was achieved by surrounding the transformer with an auxiliary sound barrier of steel plate.

Table 1 Basic Specifications

Type	Shell-form single-phase autotransformer with on-load voltage regulator
Rated capacity	3,000/3 MVA
Tertiary capacity	1,200/3 MVA
Rated primary voltage Rated secondary voltage Rated tertiary voltage	1,050/$\sqrt{3}$ kV 525/$\sqrt{3}$ kV 147kV
Tapping range	27 taps for voltages in the range of 986.6/$\sqrt{3}$ ~ 1,133.6/$\sqrt{3}$ kV
Test voltages	Lightning impulse withstand voltage Primary: 1,950kV Secondary: 1,300kV AC 1.5E (1hr)~$\sqrt{3}$E (5 min)~1.5E (1hr), E = 1,100/$\sqrt{3}$kV
Impedance	18%
Cooling method	Forced-oil, forced-air
Noise level	65dB

Construction

The 1,000kV transformer has twice the voltage and twice the capacity of 500kV transformers, which are the largest currently in use in Japan. Space constraints in shipping and installation require that the shipping dimensions be no larger than that of a 500kV transformer. We therefore chose to divide a one-phase transformer into two units, each unit having the same capacity of a 500kV 1,500/3MVA trans-

**Eiichi Tamaki is with the Ako Works and Yoshibumi Yamagata is with Tokyo Electric Power Company.*

former. The two units are designed to be connected in parallel by a T-type connection duct with an oil-gas bushing.

The 1,000kV transformer must withstand twice the voltage of a 500kV transformer and tolerate the minimal insulation distances absolutely necessary to meet transport limitations. This was achieved by designing the coil arrangement and insulation construction to reduce the electrical field concentrations, and by arranging numerous barriers to suitably divide the oil space. Cleaner manufacturing processes were also used, thus reducing the particle content in the transformer oil contributing to wider insulation margins.

Since the insulation of the 1,000kV leads would be unacceptably large if only insulating paper were used, a multilayer barrier is also applied to reduce the insulation clearance from the lead to the tank.

Fig. 1 shows the rail transport limitations, Fig. 2 the two-unit construction, and Fig. 3 the wiring connection diagram.

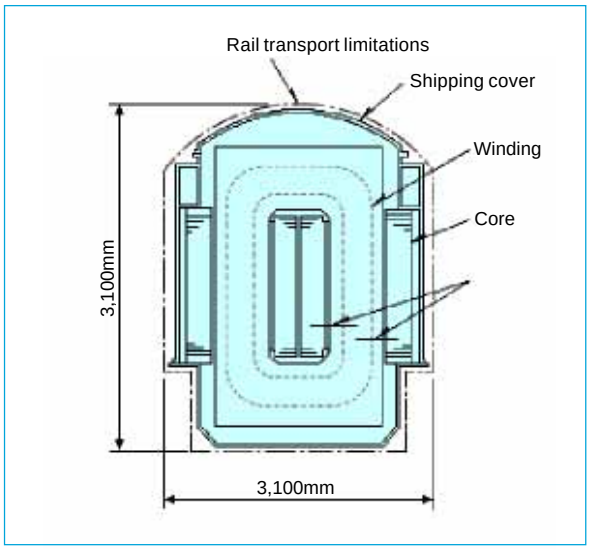

Fig. 1 Rail transport constraints.

Manufacture and Testing

Full-size models of the winding insulation, lead insulation and a prototype transformer were tested to establish 1,000kV equipment technologies. A 1,000kV, 3,000/3MVA transformer for TEPCO was manufactured following the 1,000kV technologies. All manufacturing processes from component production upward were reviewed from the standpoint of cleanliness, and cleaner technologies were introduced.

The completed transformer passed routine tests, an extreme temperature-rise test, an insulation withstand test, a static-electricification test and trial docking of the two-unit assembly.

Shipping and Assembly

The cooling unit, conservator and other exter-

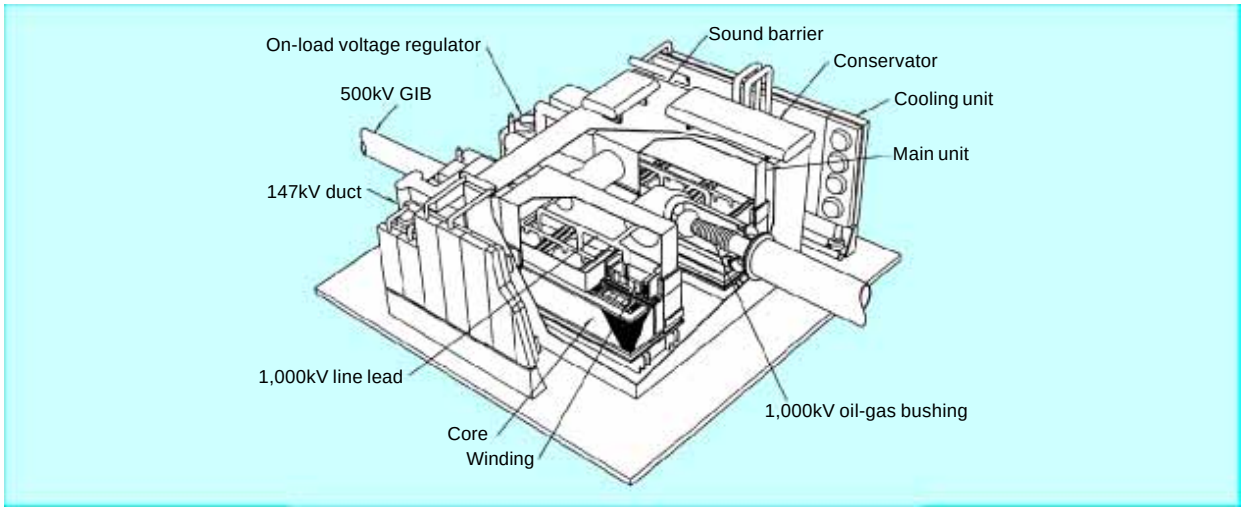

Fig. 2 Transformer construction.

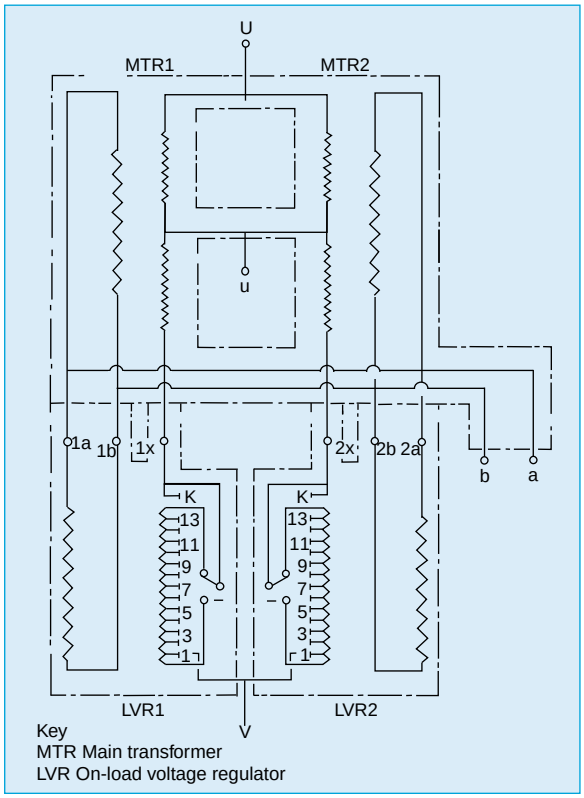

Fig. 3 1,000kV transformer wiring connection diagram.

nal components were removed, and the transformer units were filled with a low dew-point gas for the approximately 1,000km trip by ship, rail and trailer to the installation site. The shipping weight was about 200 tons, and shipping dimensions were about 3m in width, 4m in height and 8m in length.

Fig. 4 shows the unit docking procedure. The units were moved over slide rails onto a common base frame (Fig. 4a and 4b), and then positioned on the base by locators attached at the factory. The shipping cover for unit 1 was then removed, and the upper tank of unit 1 attached (Fig. 4c). The ducts were then attached using the locating pins mounted at the factory (Fig. 4d). The upper tank of unit 2 was then mounted, and unit 2 connected to the ducts using the locating pins (Fig. 4e).

The primary and secondary leads were joined to the T-duct leads, and the multilayer barrier insulation applied for the lead connection points.

The same clean procedures and thorough quality control management as that used in factory assembly were maintained during the attachment of external components and filling

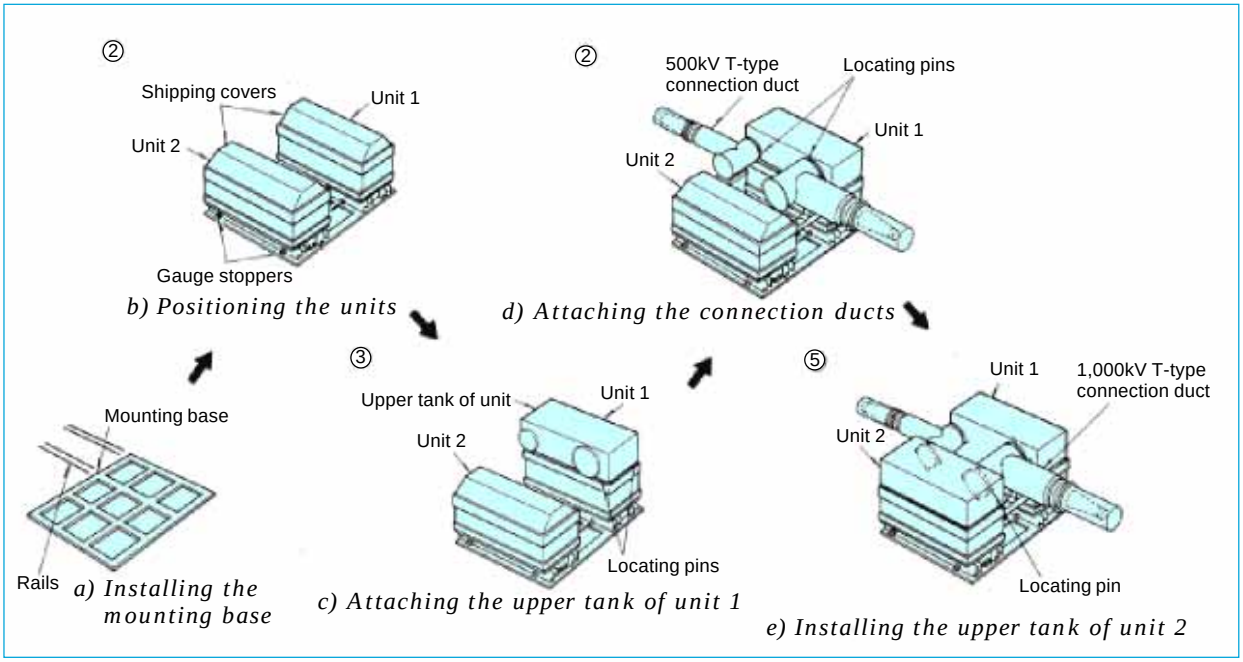

Fig. 4 Unit docking procedure.

Fig. 5 The 1,000kV transformer installed on site.

of the transformer oil.

The assembled transformers were checked for transformer ratio, polarity, winding resistance, impedance and insulation resistance. No problems developed throughout design, manufacture, shipping and assembly. Fig. 5 shows a photo of the completely assembled transformer.

Qualification Testing

The primary, secondary and tertiary terminals of the 1,000kV transformer were connected to the gas-insulated bus, and then each 1,000kV transformer was connected, in a three-phase configuration.

The secondary terminal was connected to an actual grid, and the primary opened. The temperature-rise test was conducted under the condition of partial shutdown of cooling equipment by using the tap difference between the two LVRs for units 1 and 2.

An inrush test was conducted by switching a circuit breaker connected to a 500kV line.

In the static-electrification test, the leakage current was measured at the neutral terminal with all cooling equipment running. The leakage current was sufficiently small.

Now that a 1,000kV transformer for long-term energized field testing has been manufactured and tested, commercial use of these transformers is a tangible reality. Through the above-mentioned tests, the long-term reliability of the transformers will be established over two years. The 1,000kV transformer development, manufacture, transport and assembly technologies can also be applied to improve the quality of 500kV-and-lower voltage transformers. ❑

Development of a 1,000kV SF_6 Gas Circuit Breaker

*by Takashi Yonezawa, Tsutomu Sugiyama and Mikio Hidaka**

1,000kV power transmission lines require overvoltage protection so that insulation requirements can be held to reasonable levels. Mitsubishi Electric has developed 1,000kV gas circuit breakers (GCBs) to keep switching surge levels low enough so that ground fault surges do not rise above the maximum suppressible level of 1.6~1.7 per unit (pu). The new GCBs control closing surges using a resistance creation method similar to that developed for the corporation's 550kV GCBs and prevent opening surges with a newly developed resistance interruption method. New technologies for the resistance-interruption GCB include resistance interrupters, a resistor array 15 times larger than that in 550kV GCBs, and a delayed operation function to open the resistance interrupters at a specified interval after the main interrupters open.

Development

The development team faced two major issues. The first issue was to maintain reliability in the largest and heaviest interruption equipment ever developed, including a breaker unit with the world's largest capacity to date, and a hydraulic operating mechanism specially developed for operating the main interrupters.

The second was to develop new technologies for resistance creation and resistance interruption. Fig. 1 shows the operating sequence and Table 1 lists the ratings for the 1,000kV GCB. Two operating mechanisms for the main and resistance interrupters are used, and a new delayed operation function was developed so that the resistance interrupters open after the main interrupters.

Another development issue was to design the breaker, resistor array and other elements as independent units that could be easily assembled, and to raise assembly reliability by eliminating the need for adjustments after the units are united inside the enclosure.

Features

Fig. 2 shows the internal construction. The enclosure diameter was reduced by placing the main and resistance interrupters (two sets each)

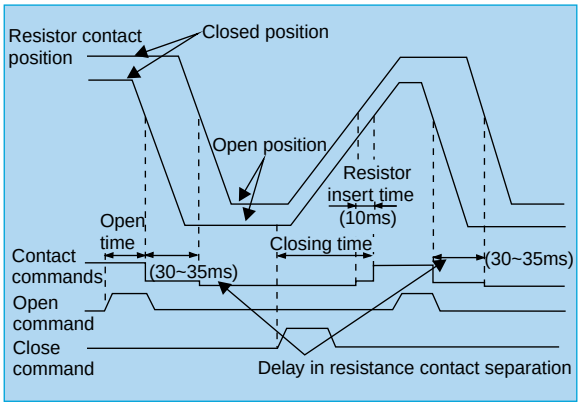

Fig. 1 Operation sequence.

Table 1 Ratings

Rated voltage	1,100kV
Rated current	8kA
Rated interrupt current	50kA
Rated interrupt time	2 cycles
Rated fluid operating pressure	31.5MPa (hydraulic)
Rated SF_6 gas pressure	0.6MPa
Resistance	700 ohms (operating and closing)
No. of breaks	2

in parallel at the enclosure center with resistors at either end. We minimized the transfer of mechanical stress from the resistors to the interrupter by mounting the resistor units on specially-developed large-diameter insulators

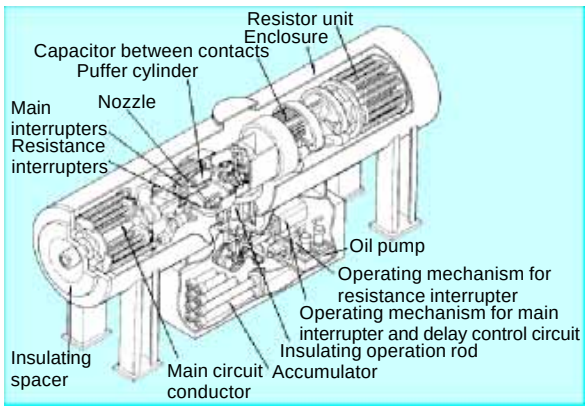

Fig. 2 Construction.

**Takashi Yonezawa, Tsutomu Sugiyama and Mikio Hidaka are with the Itami Works.*

a) Resistor unit *b) Interrupt unit*

Fig. 3 Components.

attached to the ends of the enclosure. The tulip contacts of the main and resistance interrupters are used to make adjustment-free connections between the resistor units and the interrupt unit, which eliminates all adjustments inside the enclosure. Fig. 3 shows a resistor unit and the interrupt unit.

The main contacts open at a speed just 30% faster than the two sets of main contacts used in the 550kV GCB. The speed was kept down by using a long Laval nozzle designed to maintain the hot-gas flow in a cohesive stream at high flow rates, and by optimizing the puffer cylinder diameter for maximum flow rate. The main interrupters had already been qualified in a 550kV, 63kA, one-break GCB.

The resistance interrupters require excellent dielectric recovery characteristics. With a maximum interrupting current of 2kA under out-of-phase breaking, the duty of the resistor contacts is considerably less than the main interrupters, however, the transient recovery voltage reaches a rate-of-rise of 3kV/μs during terminal fault breaking, and the peak voltage reaches 2,515kV during small capacitive current breaking—demands similar to those on the main interrupters.

For these reasons, we selected the same high breaking speed used for the main interrupters, and developed and qualified a new interrupt technology employing the small-diameter puffer of a 72kV GCB with a rotary arc drive effect achieved by permanent magnets.

The resistors typically dissipate 145MJ of energy from O to BO (i.e., terminal fault breaking to out-of-phase creation and breaking). This is 15 times the power dissipated during resistance creation of a 550kV GCB, and the large size of these resistors is a major factor in the size increase required for the 1,000kV GCB.

Fig. 4 shows the resistor configuration. The resistors are placed around the conductor connected to the main interrupters; with three resistors connected in series to form one block, and eight blocks connected in parallel. This configuration ensures adequate insulation between the resistor elements and between the resistor blocks while occupying minimum space.

The hydraulic operating mechanism for the main interrupters uses a new design to provide the necessary output, which is double the output required of the 550kV GCB operating mechanism. The operating mechanism for the resistance interrupters is the same one proven for 300kV GCBs. A hydraulic pressure stabilization mechanism prevents variations except momentarily during contact closing and opening.

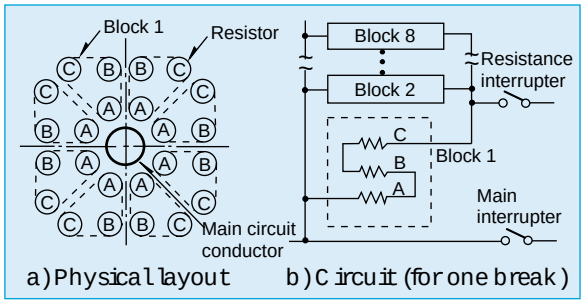

Fig. 4 Resistor configuration.

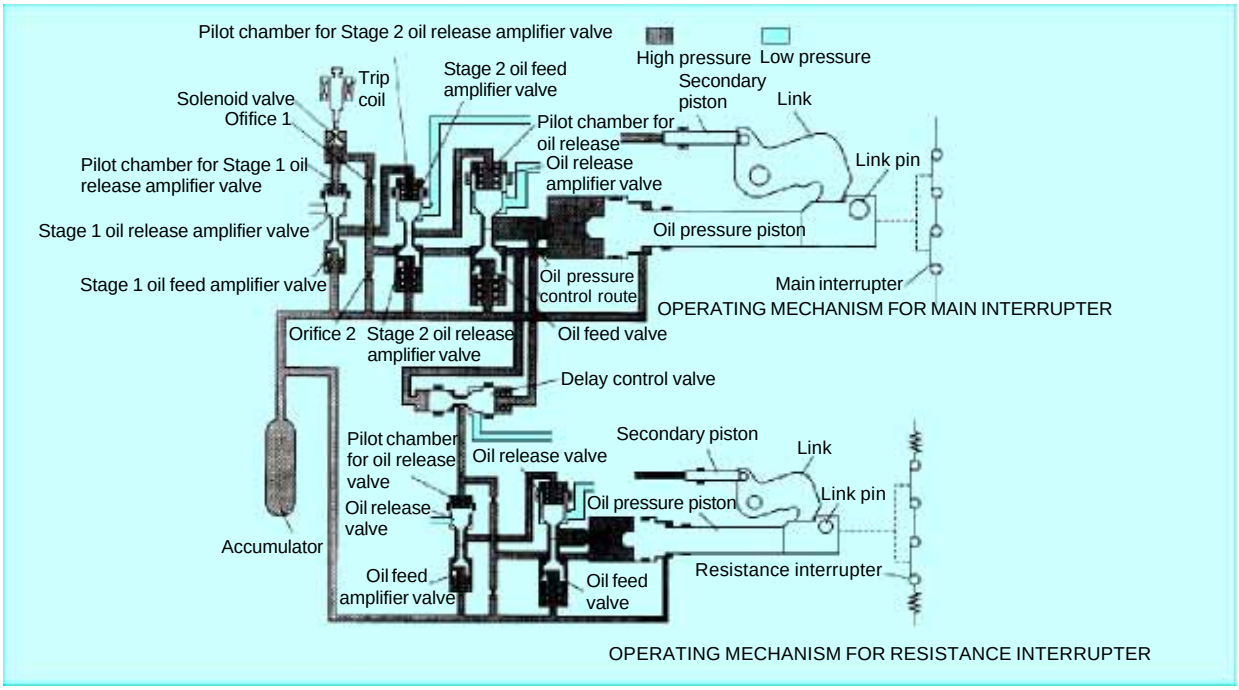

Fig. 5 Hydraulic operating mechanism and the hydraulic control circuit.

The two operating mechanisms operate with a delay when the contacts open and simultaneously when the contacts close. This function is implemented using hydraulic circuits for reliability. When the piston of the operating mechanism for the main interrupters reaches a breaking point, the dashpot pressure is detected, activating a delay control valve that triggers the operating mechanism for the resistance interrupters. Fig. 5 shows the relevant parts of the hydraulic circuit.

Verification Test

The basic performance parameters of the 1,000kV GCB have been qualified and the equipment approved for practical application.

PERFORMANCE AT EXTREME TEMPERATURES. To confirm that proper opening and closing performance is maintained at extreme temperatures, the GCB was placed in a large environment-controlled testing room and operated at temperatures from –30°C to +60°C. Fig. 6 shows that the change in opening times was negligible. The delay time of the contact separation in the opening operation of the resistance interrupter remained within the stable range of 32~33ms, confirming that the hydraulic delay circuitry is sufficiently immune to temperature-induced variations in the viscosity of the hydraulic fluid.

INTERRUPT PERFORMANCE. Limits of the test apparatus prohibited testing of the entire inter-

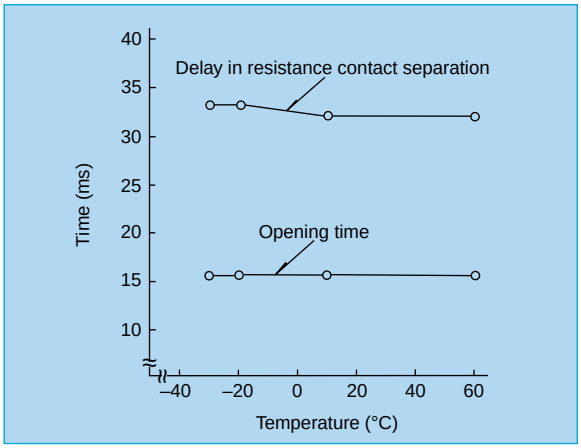

Fig. 6 Opening characteristics vs. ambient temperature.

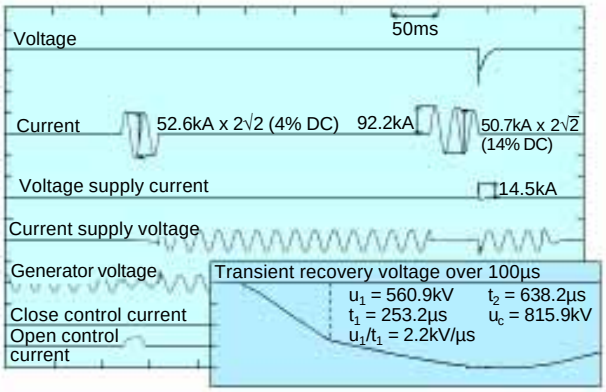

Fig. 7 Waveforms during terminal fault test for main interrupter.

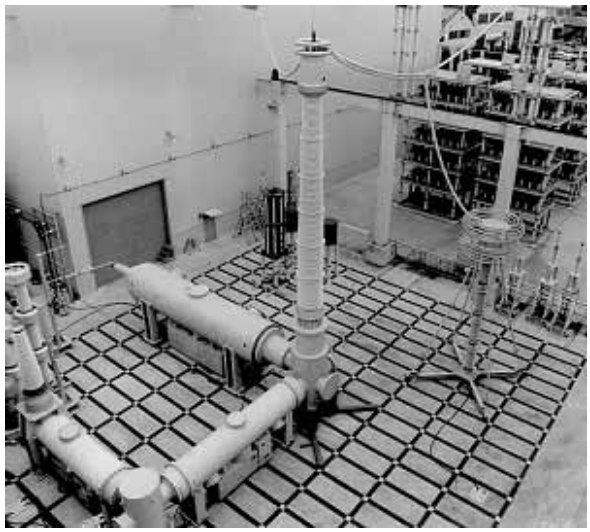

Fig. 8 Full-pole interruption test.

ruption process at once; however, selected intervals and parameters of the interruption process were tested in a multipart testing regime that covers the entire process and gives a clear picture of GCB structural and functional behaviors.

The main interrupters were tested up to the peak transient recovery voltage (TRV) with the resistors mounted normally (terminal fault duties 4 and 5), then with the resistors disconnected to allow a higher recovery voltage to be applied to the main interrupter. Fig. 7 shows waveforms for a typical qualification test during the terminal fault duty 4 test series with the resistors connected at up to the peak TRV.

The resistance interrupters were qualified for thermal and dielectric characteristics.

To check the insulation performance between the exterior environment and the enclosure, full-pole interruption tests were carried out at terminal fault duties of 4 and 5 for the main interrupters, thus causing maximum TRV (Fig. 8).

The 1,000kV GCB was installed at the Shin-Haruna UHV Equipment Test Station of Tokyo Electric Power Company in 1994. Long-term voltage and current tests began in 1995 and are still underway. ❑

1,000kV Gas-Insulated Switchgear

*by Takayuki Kobayashi, Hiroshi Yamamoto and Kenji Sasamori**

Mitsubishi Electric has successfully suppressed switching surges and lowered the required lightning impulse withstand voltage in 1,000kV gas-insulated switchgear (GIS), allowing the reduction of equipment dimensions. A high-speed ground switch supports high-speed reclosing operations, and other steps have been taken to improve grid protection and increase reliability. The equipment is undergoing qualification testing at the Shin-Haruna Substation of Tokyo Electric Power Company.

Major Features

The design of this 1,000kV GIS is based on the corporation's proven successes with its long-running 500kV equipment.

REDUCED LIGHTNING IMPULSE WITHSTAND VOLTAGE. A high-performance lighting arrestor reduces the required lightning impulse withstand voltage. This eases the insulation requirements, permitting a substantial reduction in equipment size.

Interrupt surge voltages, which do not impact the insulation design of the 500kV GIS, become significant factors at 1,000kV. We minimized these surges by developing resistance-interruption technology.

HIGHT-SPEED GROUND SWITCH. High-speed multiphase reclosing within a second window is needed to maintain grid stability when a transmission line ground fault occurs. Ground faults in a 1,000kV system induce secondary arcs in healthy phases that current reclosure systems cannot extinguish within the required period. A high-speed ground switch was developed to solve this problem. The switch closes and opens while the circuit breaker is reclosing so that the secondary arc is positively extinguished.

SIZE REDUCTION. Table 1 lists the rated and minimum gas pressures for guaranteed operation of the various equipment. The circuit breaker and high-speed ground switch employ the 0.6MPa pressure used in single-point 500kV gas circuit breakers. The other equipment employs the 0.4MPa pressure used in other 500kV switchgear. The minimum pressure for guaranteed operation in this equipment has been raised from 0.3MPa to 0.35MPa to permit higher electric field strengths and a more compact equipment design.

Table 1 Gas Pressure (MPa)

Voltage	500kV		1,000kV	
Ratings	Rated	Min.	Rated	Min.
Circuit breaker, high-speed ground switch	0.5	0.4	0.6	0.5
Other equipment	0.4	0.3	0.4	0.35

IMPROVED RELIABILITY. Free metal particles in the enclosure pose a much greater problem in 1,000kV equipment due to the high operating stresses involved. We used a dielectric coating on the inner surface of the enclosure that raises the allowable electric field strength on the surface and suppresses the movement of metal particles, thus permitting a smaller enclosure diameter.

LINEAR-COUPLED CURRENT TRANSFORMER. Fault currents in 1,000kV systems will cause core-type current transformers to saturate because the time constant of the DC component of the fault current is larger than that in 500kV equipment. The linear-coupled current transformers we employed for 1,000kV bus protection are immune to saturation.

OPTICAL VOLTAGE TRANSDUCER. Optical potential devices are used in place of previous winding-type voltage transducers because they are smaller, less expensive, have a simpler relay interface and match well with the fiberoptic LAN-based digital control and protection system.

Equipment

Table 2 lists the switchgear specifications, Fig. 1 shows the construction, and Fig. 2 is a photo of the equipment as installed at the Shin-Haruna Substation.

CIRCUIT BREAKER. The puffer cylinder diameter

**Takayuki Kobayashi is with Tokyo Electric Power Company, and Hiroshi Yamamoto and Kenji Sasamori are with the Itami Works.*

and stroke have been optimized and the nozzle configuration improved, making it possible to achieve sufficient performance from two series-connected 500kV interrupters.

The resistance creation method developed for 500kV gas-circuit breakers is now complemented by a resistance interruption method. The 700Ω interrupters are the same type used in the 500kV equipment, with eight elements connected in parallel to handle the greater energy duty.

Hydraulically driven operating mechanisms operate the main and resistance interrupters. The delay required in opening the resistance interrupters is provided by the hydraulic circuit, which is designed to keep the delay time variations within a couple of milliseconds.

Table 2 Specifications of 1,000kV GIS

All equipment	Rated voltage	1,100kV
	Rated current	8,000A outside of bank circuit 2,000A in bank circuit
	Short-time withstand current	50kA, 2s
	Lightning impulse withstand voltage	2,250kV
	Power frequency withstand voltage	1.5E x 30m – $\sqrt{3}$ x 1m – 1.5E x 30m (E=1,100/$\sqrt{3}$kV)
	Rated gas pressure	0.6MPa in GCB, HSGS, 0.4Mpa in other equipment (at 20°C)
Gas-circuit breakers	Rated breaking current	50kA
	Rated operating sequence	Standard O – θ – CO – 1m – CO (θ = 1s)
	Operating mechanism	Hydraulic
	No. of breaks	2
	Break/make system	Resistance interruption, resistance creation (700Ω)
Interrupters	Surge control system	Resistance insertion (500Ω)
	Loop current switching	8,000A
	Operating mechanism	Motor-charged spring
Earth switches	Line-charging current switching	50kV, 40A electrostatic, 70kV, 1,000A electromagnetic
	Operating mechanism	Motor-charged spring
High-speed ground switches	Line-charging current breaking	1,200A electrostatic, 7,000A electromagnetic
	Rated operating sequence	C – θ – O (θ = 0.5s)
	Operating mechanism	Hydraulic
Insulated bus	Rated current	8,000A outside of bank circuit 2,000A in bank circuit
Surge arresters	Rated voltage	826kV
	Protection level	1,620kV, 20kA
	Energy absorption capability	55MJ
Current transformers	Type	Core type Linear-coupled type
	Accuracy class	Class 1.0 1.0%
Voltage transformers	Type	Optical potential device
	Accuracy class	Class 1.0
Bushings	Type	Gas bushing
	Pollution withstand voltage	762kV

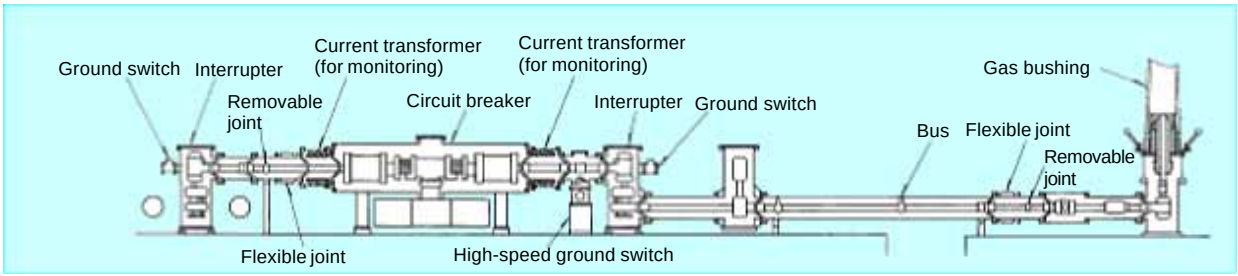

Fig. 1 The construction of 1,000kV gas-insulated switchgear.

Fig. 2 A photograph of 1,000kV GIS installation.

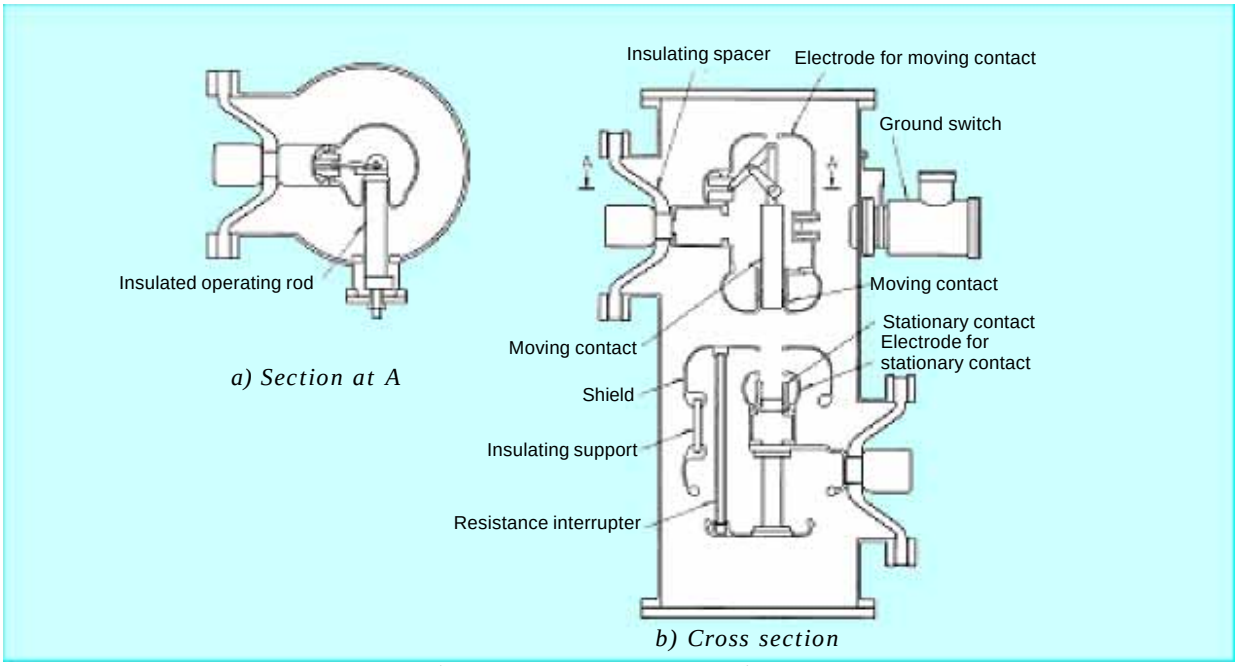

Fig. 3 Interrupter construction.

INTERRUPTER. Fig. 3 shows a diagram of the interrupter. Like its 500kV predecessor, the fixed interrupt and moving interrupt mechanisms are supported by space-efficient insulating spacers. Use of a rotary-drive insulated operating rod permits a compact, upright design that can be trans-

ported as a single unit.

The surge-suppression interrupter is made of the same carbon ceramic element used in the circuit breaker (Fig. 4). The simple cylindrical shape allows manufacture by simpler, more stable processes. The contacts for the interrupter are grouped on the side where the interrupter is fixed. This space-saving configuration contributes to a smaller enclosure diameter.

Table 3 lists the duty of the surge-suppression interrupter. While the energy duty is small at 25kJ, the 1,700kV withstand voltage is high, and this voltage must be withstood repeatedly. Various interrupter models were tested to arrive at a design capable of enduring 2,000 surges without destruction or resistance change. The interrupter elements are approximately 1m long, and four elements are connected in parallel.

The contacts have been designed with an electrical field distribution so that a reclosing arc forms between the moving contact and the interrupter shield.

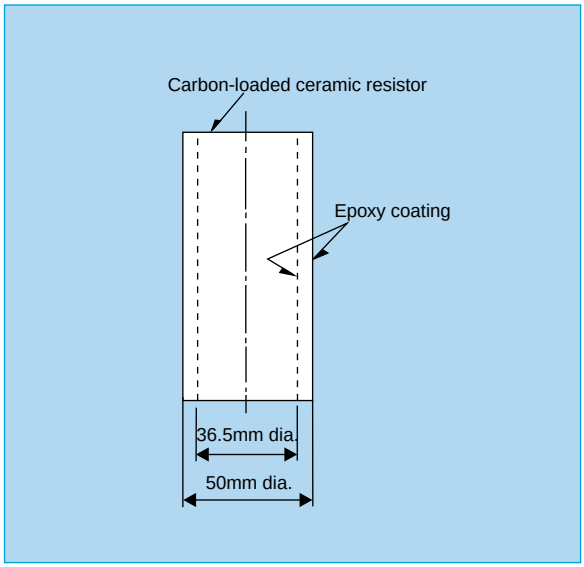

Fig. 4 Surge-suppression interrupter construction.

HIGH-SPEED GROUND SWITCH. Fig. 5 shows the construction of the high-speed ground switch. To save space, the fixed contact has been placed on the main horizontal conductor leading to the circuit breaker with the moving contact directly below. A hydraulic operating mechanism placed below the contacts drives the high-speed opening and closing action.

The high-speed ground switch breaks the line charging current after the circuit breaker opens for a single-line ground fault. Furthermore, if another phase fault should occur while the high-speed ground switch is operating, the switch is designed to interrupt the no-zero-passage currents for 80ms.

In puffer-type interrupters, the puffer pressure is usually highest while the contacts are opening, and falls quickly after the contacts are fully open. However in this application, interrupting the long arc caused by a no-zero-passage current requires a longer puff time, which necessitates an increased puffer dead volume after the contacts open, and that the puffer pressure should drop more gradually.

Fig. 6 shows that the dead volume needs to be increased nine times to ensure a puff time of at

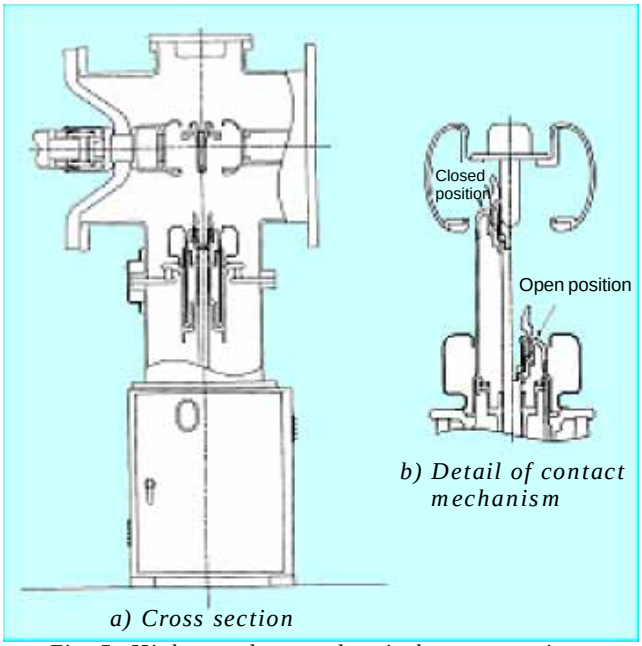

Fig. 5 High-speed ground switch construction.

Table 3 Surge- Suppression Interrupter Duty

Withstand voltage		1,700kV
Energy duty	Open	10kJ
	Close	15kJ
	Close, open	25kJ

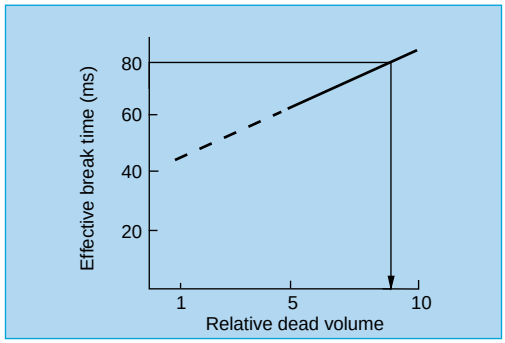

Fig. 6 Effective break time vs. relative dead volume of puffer cylinder.

least 80ms. We achieved this by doubling the puffer cylinder diameter.

Large surges can appear in the ground conductor if secondary arcs accompany high-speed ground switch opening or closing. We minimized this likelihood by improving the insulation performance of the insulating spacers, and by arranging plural grounding plates to short the ground terminal to the enclosure, which prevents a rise in the ground conductor potential.

We verified the efficacy of this design by testing it at 640kV to simulate a transient recovery voltage during the interruption of an electromagnetic induction current. No practical problems arose. Some 40% of the applied voltage (240kV) appeared between the ground conductor and enclosure, and 5% (32kV) between the ground terminal and enclosure.

BUS INSULATION. We applied a dielectric coating to the inner surface of the enclosure to suppress the removal stress caused by the metal particles on the conductor. This allows the electric field strength on the inner surface of the enclosure to be boosted from the 0.9kV/mm value in 500kV equipment up to 1.2kV/mm (Fig. 7), with the result that the busbar enclosure diameter could be reduced to 900mm (Fig. 8.) The GIS was designed to tolerate the presence of metal particles in the enclosure up to 3mm long and 0.2mm in diameter.

EXTENDED INSULATOR TESTING. High electric fields can potentially damage insulators over time, so we conducted long-term testing at commercial power supply frequencies on sample insulators. We found that degradation was negligible at field strengths of 12kV/mm or less,

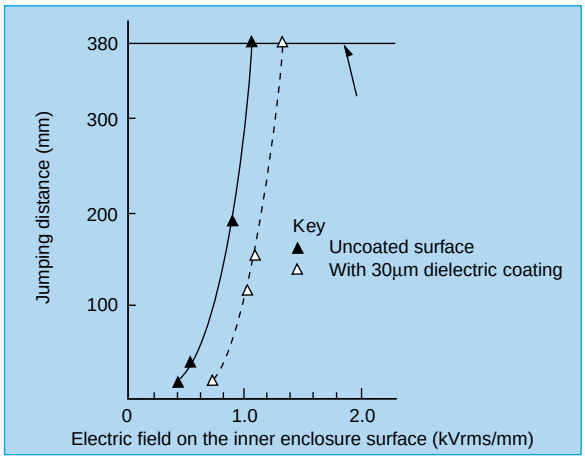

Fig. 7 Jumping distance of particles on the enclosure's inner surface. The test particles are 3mm long and 0.2mm in diameter.

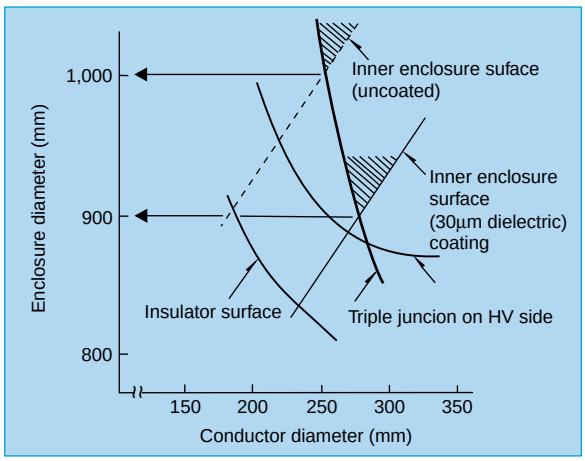

Fig. 8 Parameters influencing gas-insulated bus design.

indicating a substantial margin for tighter design standards. We therefore chose to boost the allowable stress on insulating spacers by 20%.

A conservative approach based on technologies proven at 500kV has enabled Mitsubishi Electric to develop 1,000kV gas-insulated switchgear with assured performance for the next generation of high-capacity low-loss power-transmission systems. ❑

A Protection and Control System for 1,000kV Power Transmission

*by Takayuki Matsuda, Shin'ichi Azuma and Masaji Usui**

Mitsubishi Electric participated in the joint development of a 1,000kV protection and control system, which is undergoing qualification testing at the Shin-Haruna Substation of Tokyo Electric Power Company. The transmission line protection system features an improved charging current compensation system and newly developed multiphase reclosing with high-speed grounding and arc suppression technology. The busbar protection system features the application of a linear-coupled current transformer, and transformer protection includes a newly developed current comparison relay.

Fig. 1 Outdoor cubicles housing a 1,000kV substation protection and control system.

Configuration

A number of protection and control issues must be solved before future 1,000kV power transmission systems can enter routine service. Due to the increased charging current and larger diameter of the transmission-line conductor, faults result in the generation of transients with low-order harmonic numbers, AC overvoltage conditions and longer DC transients. Tokyo Electric Power Company, Mitsubishi Electric and two other electrical equipment manufacturers have jointly developed a protection and control system for 1,000kV lines that addresses these issues.

Fig. 1 shows a photo of the system, which is housed in two 2,990mm-wide cubicles. Fig. 2 shows a diagram of the system configuration.

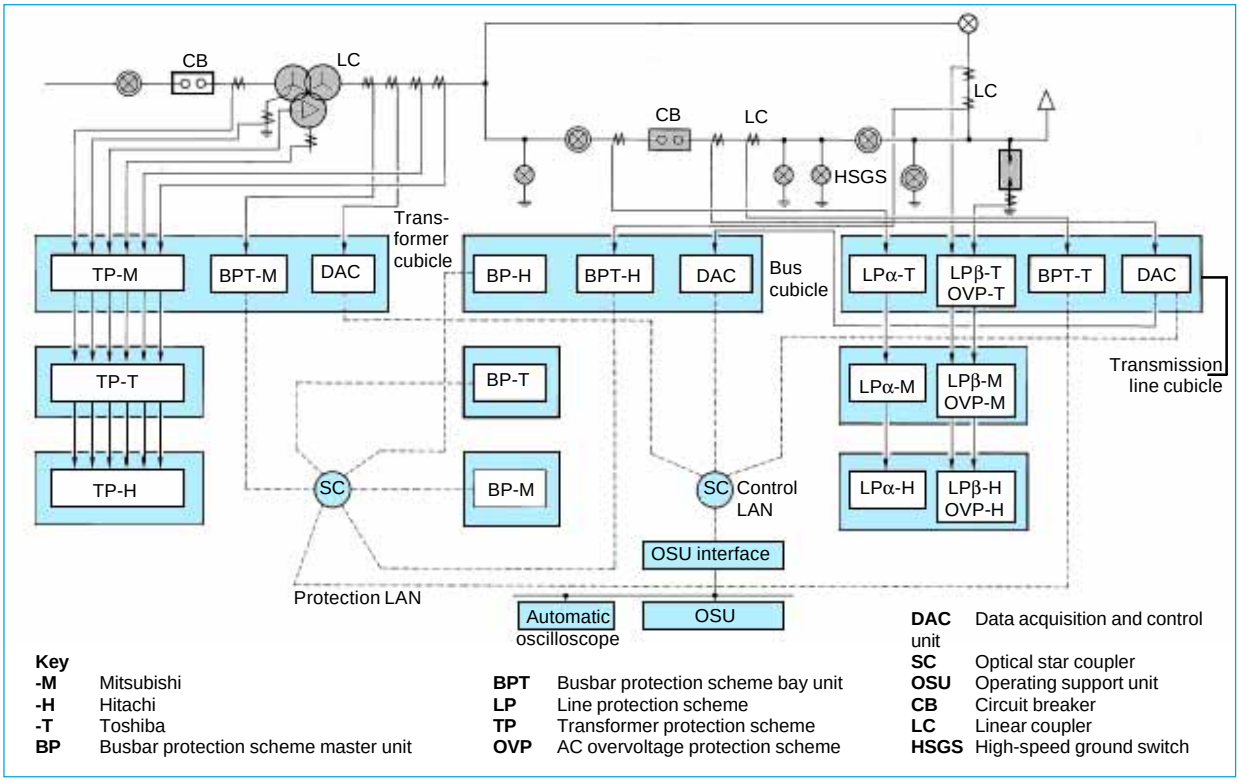

Fig. 2 System configuration.

**Takayuki Matsuda is with Tokyo Electric Power Company, Shin'ichi Azuma with the Power & Industrial Systems Center and Masaji Usui with the Power System & Transmission Engineering Center.*

Mitsubishi Electric oversaw development of the transformer cubicle, which includes 1,000kV transmission protection, busbar protection, transformer protection, AC overvoltage protection, a data acquisition and control unit, and the signal processing unit of the optical voltage transformer.

In the busbar protection system, a fiberoptic LAN connects the master units and the bay units of each manufacturer. The master units perform a protective function while the bay units monitor the current transformer outputs and switch conditions, and execute circuit-breaker trip functions.

In the control system, a fiberoptic LAN links the control terminals of each manufacturer, operation support units and the automatic oscilloscope. The system supports equipment control, equipment status monitoring, instrumentation and fault indication functions.

Optical PCM communications between the protection and control systems support relay setting, switching control and alarm indications.

Features

TRANSMISSION-LINE PROTECTION. The lower fault-detection sensitivity associated with increased transmission-line charging current has been addressed by improved charging current compensation for the current differential relays. More sophisticated reclosing functions have also been developed.

In charging current compensation schemes to date, the voltages at individual terminals are used to calculate the charging currents between them, and 100% of these values are used for compensation. In such schemes, the maximum per phase error current is 1.5 times the transmission-line charging current in the case of open-circuit faulting of a voltage transformer secondary circuit; therefore, the sensitivity of the current differential relay must be decreased to prevent misoperation in 1,000kV systems. We successfully halved the error by transmitting the local current data with a 50% compensation of the charging current using local voltage data to the remote terminal, thereby satisfying the sensitivity for fault detection.

Due to the system's increased charge capacity, large induced voltages from unfaulted phases can delay suppression of secondary arcs in the dead time during high-speed automatic reclosing, and prevent reclosing within the required one-second interval. We solved this problem by inserting high-speed ground switches in the power system. Switches on each end of the faulted phase activate immediately after the circuit breaker opens, extinguishing the secondary arc. The switches are then opened and the circuit breaker reclosed. Fig. 3 shows oscilloscope traces from a reclosing test conducted at the factory site. In this case, a fault in phase 'a' extends to phase 'b'. Both phases independently trip and reclose.

BUS PROTECTION. Fault currents in 1,000kV systems result in DC transients of a long duration that saturate core-type current transformers and lead to misoperation of current-differential relays. We therefore changed over to linear-coupled current transformers that do not saturate. We chose a high secondary impedance since linear-coupled current transformers have the same permeability as air and excitation impedance is low.

The secondary output of these transformers is proportional to the primary current and saturation does not occur. The secondary circuit does not open at abnormally high voltages like the core-type circuit. There is a trade-off, however, since the magnitude of harmonic current components in the output increases proportionally with harmonic order. Because the output is dependent on the differential of the primary current, the secondary voltage is proportional to the frequency and the phase advances by 90°.

We simulated the fault current waveform for a power system that is prone to harmonic generation, and verified the correct relay response. We triggered a fault on a model transmission line and found the correct relay response against low-order harmonics. Finally, we connected a field specification linear-coupled current transformer, and verified the relay operation using a short-circuit generator to simulate internal and external faults.

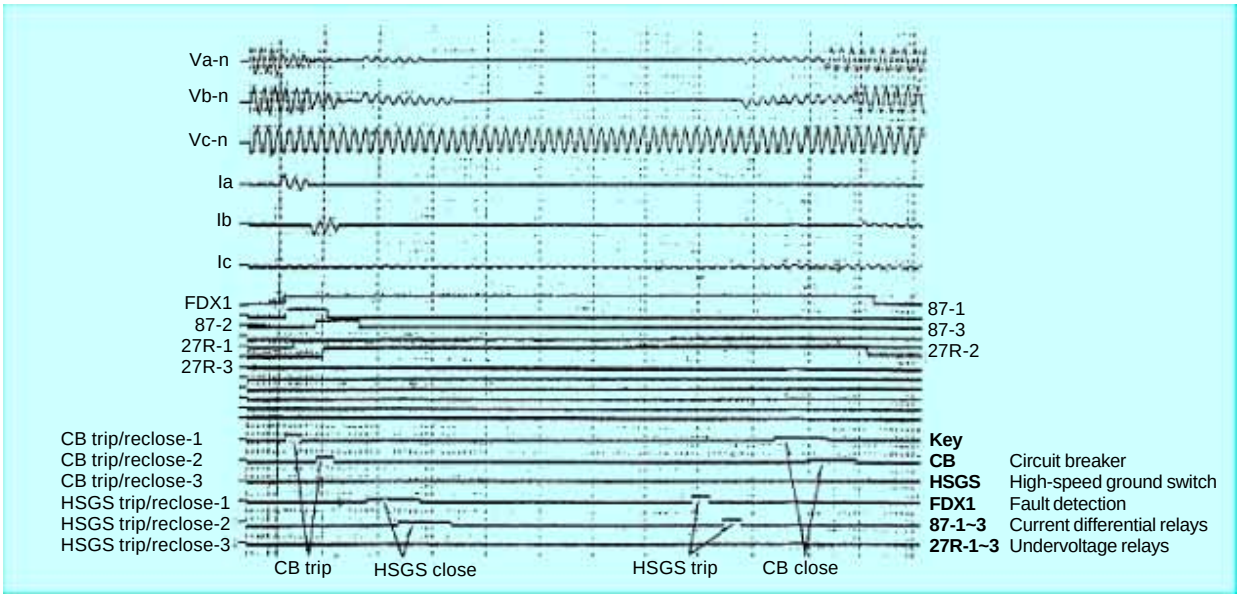

Fig. 3 Oscillograph of multiphase reclosing in high-speed grounding and arc-suppressing system.

TRANSFORMER PROTECTION. Successful transformer protection in 1,000kV systems requires a method to distinguish transformer faults, which have strong low-order harmonics, from excitation inrush currents, and to adjust to the proportionally lower transformer fault currents to higher system voltage and transformer capacity. We addressed these issues by placing current comparison relays between the enclosures and current differential relays between the transformer primary, secondary and neutral points. Fig. 4 shows the configuration of a 1,000kV transformer and the current transformer arrangement that protects it.

When phase faults occur in the series, shunt or tertiary windings, an imbalance occurs in the current between the two enclosures. Since normal loads and excitation inrush currents are well balanced, faults are identified by comparing the currents in the parallel windings. This method also offers enhanced sensitivity.

When ground faults occur, a current differential appears in the normally zero sum of the primary, secondary and neutral-point currents. This provides high sensitivity for ground faulting.

An excitation current flowing through the tertiary delta circuit and a terminal short are signs of a fault between phases. Current differential protection is therefore placed on the tertiary delta circuit.

We manufactured a scale model of the 1,000kV transformer and verified the protection functions on a model transmission line. Simulated inrush currents associated with the closure of primary or secondary circuit breakers failed to cause spurious operation. We also failed to induce spurious operation by varying the enclosure connect timing, as well as varying the excitation current by about 30% to create an unbalanced inrush current.

AC OVERVOLTAGE PROTECTION. We qualified a lightning arrestor discharge current detection algorithm and high-speed transfer trip function that are used to provide AC overvoltage protection.

The lightning arrestor discharge current is detected at the local terminal in which the circuit breaker is open, and the status information is transferred to the remote terminal. The circuit breaker executes a high-speed trip at the remote terminal when an overvoltage fault is detected.

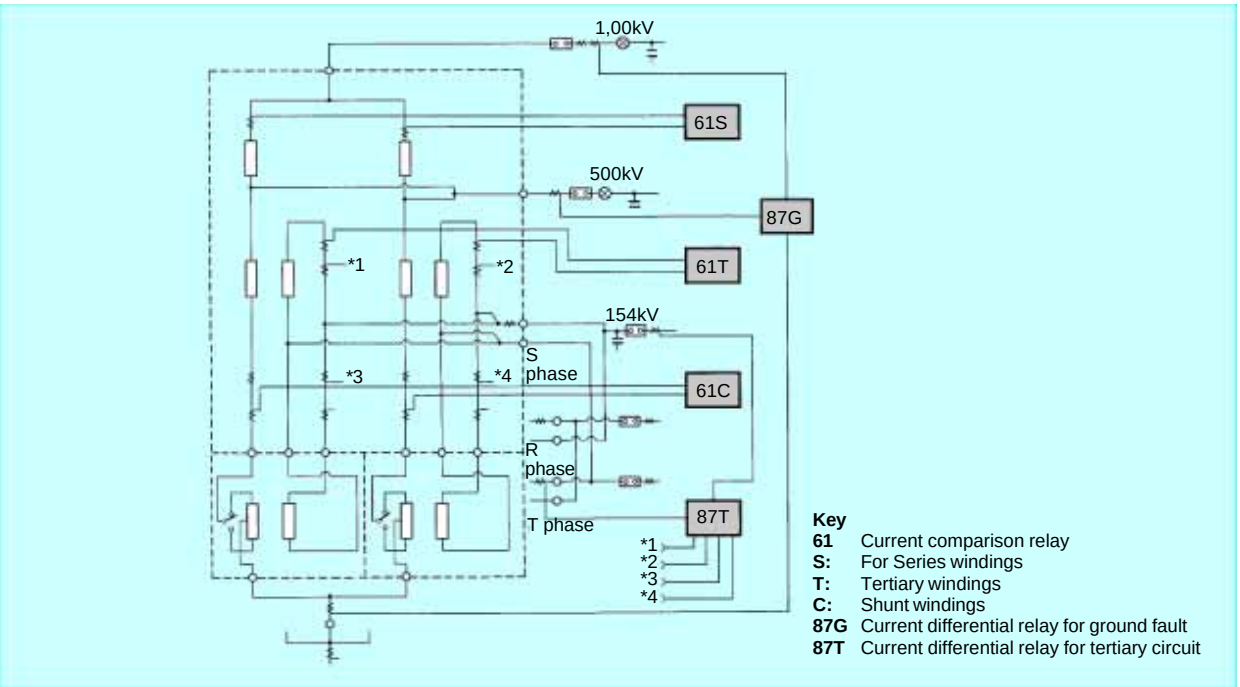

Fig. 4 Configuration of a 1,000kV transformer and the current transformer arrangement for its protection.

The main relay operates when the cumulative current through the lightning arrestor exceeds a specified threshold, and operates instantaneously when a high overcurrent is detected.

The lightning arrestor discharge waveform is triangular, and the relay operating value is determined by the average current corresponding to a triangular waveform with a 2ms base.

The time from overvoltage to arrestor destruction is minimum when the load disconnect overvoltage causes a flashover and a voltage rise in the unfaulted phases. Since arrestor destruction will occur at 90ms after a ground fault, the line circuit breaker must operate within about 80ms.

Power system protection equipment must operate to protect the system from damage due to a variety of fault conditions and maintain services with minimum interruption. The system described here meets these requirements within the stricter performance constraints of 1,000kV power systems. ❑

Simulation Technology for 1,000kV Power Systems

*by Koichirou Ikebe, Tetsuro Shimomura and Dr. Isao Iyoda**

New simulation technologies are required to understand the behavior of 1,000kV power systems and to guide the development of 1,000kV equipment. This article reports two related items: an efficient simulation method for evaluating the unbalanced voltage and current conditions that occur in non-transposed transmission lines, and a new modeling method that can precisely analyze the surge behavior of low-attenuation 1,000kV lines.

Development Background

The highest power transmission voltages, now reaching 1,000kV, are used to transport electric power long distances through overhead transmission lines. Typical Japanese power lines are configured as shown in Fig. 1. Transposition, a rearrangement of the lines to balance the line characteristics with respect to each phase, is not applied at 1,000kV due to the difficulty of insulation. Symmetrical components cannot be used to analyze sequence separation in non-transposed overhead lines due to the unbalanced transmission line constants of the non-transposed configuration. Since voltage and current imbalances originating in the transmission lines can cause generator and transformer overheating just as load imbalances do, solutions to maintain balanced operating conditions must be found. Studies are also essential because imbalances in long-distance, high-capacity 1,000kV power lines will effect entire regional power networks.

Analysis Tools for Unbalanced Lines

Most existing power network analysis programs assume balanced line and balanced load conditions. Although they can perform transient stability calculations and short-circuit current analysis for unbalanced fault conditions, they do not deal with unbalanced networks.

The Electromagnetic Transient Program (EMTP) has been used to analyze ongoing voltage and current imbalances originating in unbalanced lines, but this approach suffers several problems. First, one must set the internal voltage of the generator (i.e., absolute voltage and voltage phase angle) using other programs. Second, it is not possible to take account of the generator's negative sequence impedance, which makes it difficult to accurately calculate the generator's negative sequence current. Third, massive data input and output processing is required, which makes the program unsuitable for analyzing large networks.

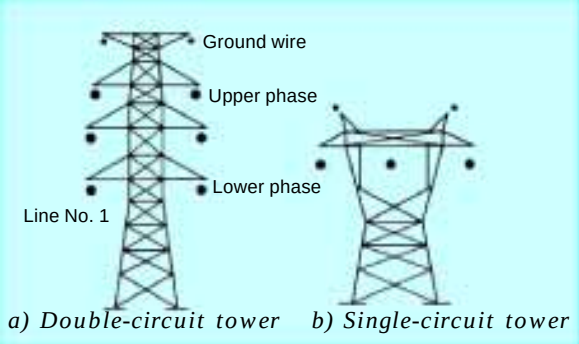

Fig. 1 Towers and disposition of lines.

We therefore developed a method for analyzing unbalanced voltages and currents arising in networks containing unbalanced transmission lines, loads and compensation devices. The method employs phase components, which are more general than symmetrical components, and unlike EMTP, which requires voltage and current source explicitly, the power equations for three phases are solved using the Newton-Raphson Method.

The program is capable of performing calculations for nearly the entire main grid of the Tokyo Electric Power Company. Verification

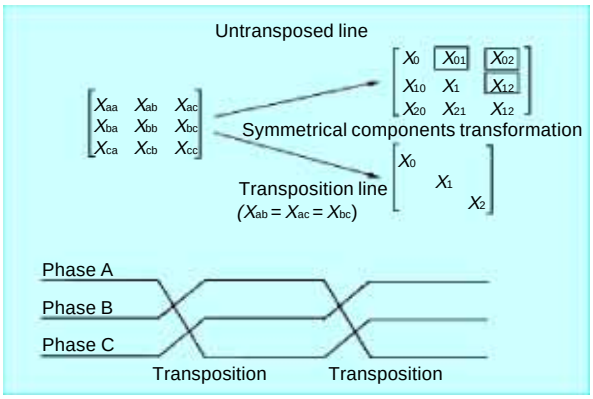

Fig. 2 Transposition and matrix of coefficients.

**Koichirou Ikebe is with Tokyo Electric Power Company, Tetsuro Shimomura is with the Itami Works and Dr. Isao Iyoda with the Power System & Transmission Engineering Center.*

testing was conducted on a model consisting of 500kV and 275kV networks including 191 buses and 109 lines. Based on this program, we have developed an additional program for analyzing fault currents generated by the many possible fault scenarios on complicated networks.

Results

The program for power flow calculations under unbalanced voltage and current conditions has already been applied to the investigation of a number of problems (e.g., analysis of negative sequence currents in generators and transmission lines, analysis of network voltage imbalances caused by the unbalanced loads of electric trains, and analysis of the behavior of new power line configurations and transpositions). Establishing a database of detailed physical information on the lines for analytical purposes has had the additional benefit of making network electrical characteristics data available. The authors plan to explore further applications in the design of 1,000kV transmission line relays, calculation of illogical harmonic current components and design of equipment to compensate for transmission line imbalances.

Transient Recovery Voltage Analysis

Transient recovery voltage (TRV) is a type of surge that occurs between opening circuit-breaker contacts.

CONSIDERATIONS IN 1,000KV LINES. 1,000kV transmission lines are long with little loss, and the system's resonant frequency is low. As a result, fault-induced transients attenuate slowly, and remain superimposed on the lines well after the fault current has been cleared and normal operation resumed. These transients also present a danger of propagating into 500kV networks.

We used the methodology presented above to analyze these phenomena and design countermeasures. We modeled a system consisting of a 1,000kV network with five substations and a 500kV network with about 30 substations, and analyzed TRVs in the 1,000kV network. Fig. 3 shows a diagram of the 1,000kV network. We used the J. Marti EMTP model for the 1,000kV lines, but the large amount of input data for the 500kV network required that we simplify it to two lines expressed as a three-phase distributed-parameter line model.

In previous analyses, the state at the time the fault occurs is taken as the initial state for calculating the voltage that occurs across the circuit breaker contacts as they open. However,

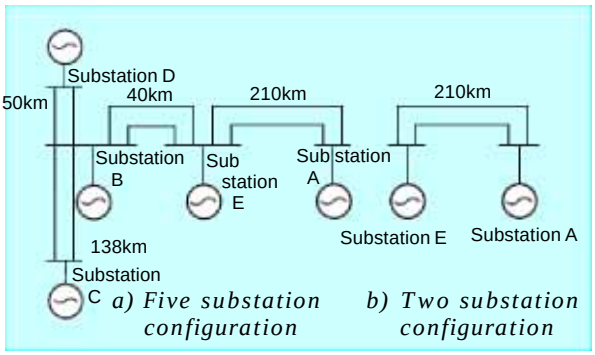

Fig. 3 1,000kV power system model.

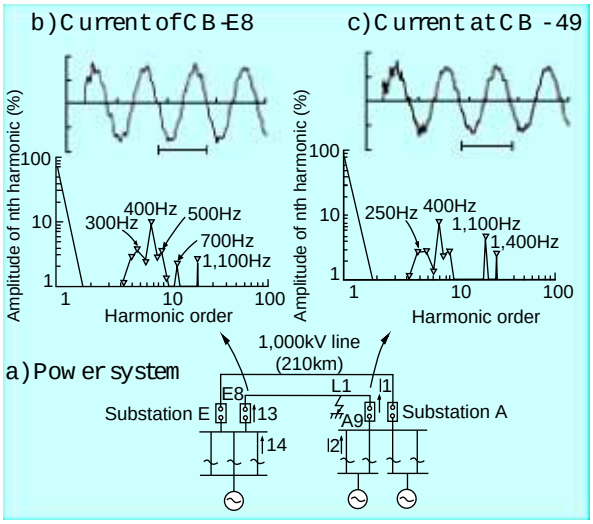

Fig. 4 A fault current waveform and its Fourier analysis.

due to the low attenuation of fault-induced harmonic components in 1,000kV systems, the pre-fault state is taken as the initial state, and the fault and fault recovery are simulated. The 1,000kV circuit breakers employ a resistive breaking method, with the resistor contacts opening 20ms after the main contacts open at the current zero point.

Our model incorporated not only the resistive loss of the lines but also the core loss and copper wire loss of the transformers, as well as fault-point arc losses. Load effects were also studied

ANALYSIS RESULTS. We performed a TRV analysis on a 1,000kV system at each stage of construction with respect to substation faults and transmission line faults. Due to the low transmission line resistance, the high-frequency currents induced by fault transients attenuate only slowly. These high-frequency components remain superimposed on the line after fault recovery, causing *di/dt*, the rate-of-change in the current, to grow large. The frequency of the high-frequency current is determined by the transmission line length—350Hz in the case of

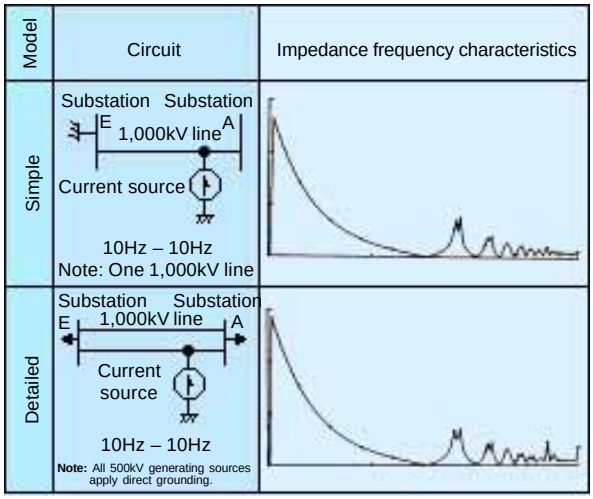

Fig. 5 Frequency characteristics of a 1,000kV power system.

a 210km transmission line. Considering the losses at this frequency in the 1,000kV lines, 500kV lines and transformers, the *di/dt* when a fault is cleared converts to an rms value of less than 50kA, which is low enough to present no problems.

STUDIES ON HIGH-FREQUENCY CURRENTS. The fault-current described above consists of several high-frequency current components. We studied the frequency response of the network and analyzed the frequency of the high-frequency currents.

We used the EMTP frequency scan command to determine the frequency characteristics of a two-substation 1,000kV network, and determined that two resonance points exist at 350 and 700Hz. We then analyzed the fault current with the EMTP Fourier on command and discovered that the largest components were at 300 and 400Hz—six and eight times the fundamental frequency. We studied the influence of the superimposed high-frequency components using the current injection method, which connects a current source at the fault point and then superimposes several high-frequency current sources and injects them onto the line. Fig. 6 shows that the results are relatively accurate. Future studies are needed to examine a wider range of harmonic frequencies.

In conclusion, our 1,000kV TRV analysis was conducted in greater detail and with modeling on a greater scale than previously implemented. The results facilitated the design of circuit breakers.

Interrupter Surge Analysis

Analysis of the interrupter surge in 500kV gas-insulated switchgear yielded a peak overvoltage of 2.8 per unit (pu) in contrast to a measured value of 2.7pu. In 1,000kV systems, a lightning impulse withstand voltage (LIWV) of 2,250kV, approximately 2.5pu, has been adopted, and surge voltages must be held within this limit. Interrupter surges are numerous, occurring every time that an interrupter opens or closes. Use of a resistive disconnect scheme keeps transients far below 2.5pu.

We analyzed the worst-case interrupter reclosing arc in a substation consisting of four circuits and four banks, assuming a 2.0pu voltage between the contacts. We modeled the system using a single-phase distributed-parameter line model, varying the bus connections and choice of interrupter at which the reclosing arc

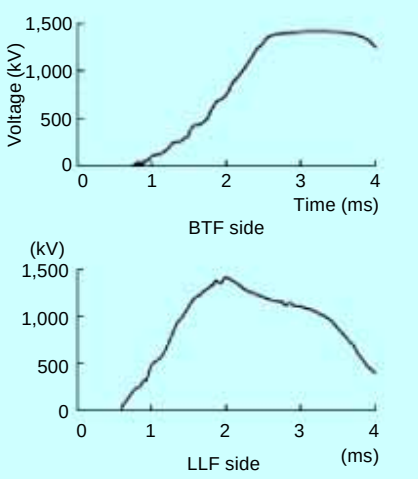

a) TRV waveform in clearing of a transient grounding fault

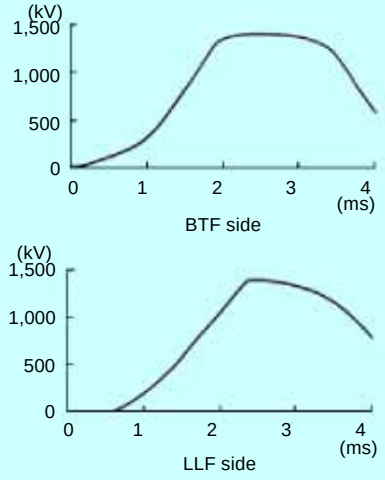

b) TRV waveform obtained from current injection simulation

Fig. 6 Results of current injection simulation.

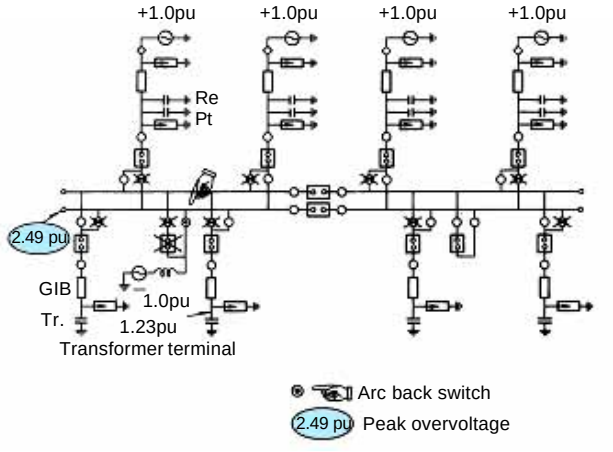

Fig. 7 Substation configuration.

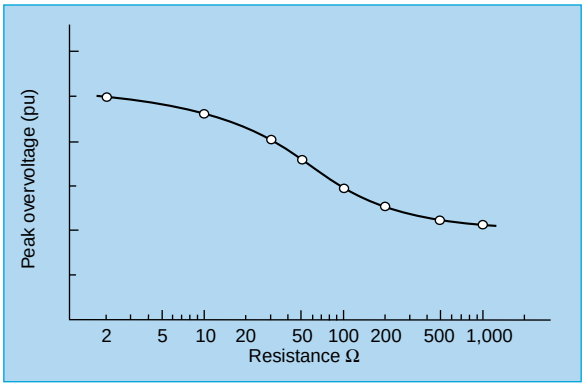

Fig. 8 Peak overvoltage ratio for various values of parallel switch resistors.

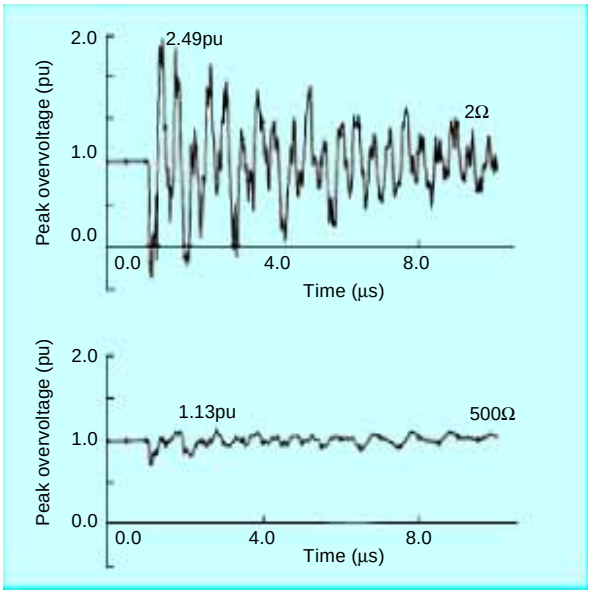

Fig. 9 Result voltage waveform (case II at gas-insulated switchgear terminal)

occurred. The value of the surge-suppression resistor was varied during the simulation from the reclosing arc resistance of 2Ω to a maximum of 1,000Ω.

Without taking special steps, the transient voltage caused by a reclosing arc at the bus interrupter reaches 2.49pu, with a surge frequency upwards of 2MHz. Fig. 8 shows the dramatic increase in the surge voltage suppression that occurs as the resistance of the parallel switching resistor increases. Fig. 9 shows the voltage waveform for a typical resistance value. In the final design, we selected a 500Ω resistance, which holds the peak transient voltage to approximately 1.1pu.

Simulation technology has played a vital role in the design of 1,000kV power systems. The technology has been developed over 20 years of experience and extensive knowledge of 500kV power systems, and promises to help simplify the daunting task of designing, manufacturing and testing large-scale power network equipment. ❑

A Monitoring System for 1,000kV Gas-Insulated Switchgear

Mitsubishi Electric has delivered a gas-insulated switchgear monitoring system for use in qualification testing of 1,000kV substation equipment at the UHV testing yard of Shin-Haruna Substation, Tokyo Electric Power Company (TEPCO). Testing has been underway since 1995.

Fig. 1 shows the system configuration. The monitoring panel receives data from sensors, which it processes and analyzes to determine the equipment status. This information is sent out over a 1:N optical HDLC LAN to an on-site control room, where it is logged and displayed. The data stream can also be routed through the video conferencing system of the TEPCO administrative offices to the Mitsubishi Electric factory. Mitsubishi Electric can also set up a personal computer and modem in the monitoring panel cubicle to send proprietary instrumentation data to the factory over a telephone line.

The system monitors the following items.

PARTIAL DISCHARGE. An internal antenna detects partial discharges. Factory testing demonstrated a maximum detection sensitivity of 0.5pc.

INTERNAL FAULT LOCATOR. This function is realized using gas pressure sensors, and is capable of detecting pressure increases of 100 pascals.

LIGHTNING ARRESTOR LEAKAGE CURRENT. A current transformer installed on the lighting arrestor ground circuit detects leakage current. The total value of the leak current components at the fundamental frequency and phase angle Δ are used to determine the resistive leakage current.

TRAVEL CHARACTERISTICS. A control current sensor, which monitors the control current run time of the control circuit, a travel sensor that directly measures movement of the operating mechanism and auxiliary contacts are used to monitor travel characteristics. Combined operation of the high-speed ground switch and gas circuit breaker can also be monitored.

HYDRAULIC PUMP OPERATING CHARACTERISTICS. The operating times and operating duty of the electromagnetic relay that powers the hydraulic pumps are monitored. This does not include pump operation associated with manually initiated equipment operation.

SF_6 GAS PRESSURE AND DENSITY. Sensors monitor gas pressure and density to identify leaks and to locate internal faults.

The equipment also monitors contact wear and lightning arrestor discharge current.

The single-panel monitoring unit is capable of monitoring a three-phase gas-insulated switchgear unit. The naturally-cooled cubicle has a protective sun shade and an internal dehumidifier. Fig. 2 shows the detailed equipment configuration. A CRT monitor enables visual monitoring of the instrumentation data and sensor operation status, and screens can be printed on demand. Data can be uploaded to a remote location via 1:N optical HDLC LAN or via modem over telephone lines. The data received from this equipment will be analyzed and used to design future gas-insulated switchgear and related monitoring equipment. ❑

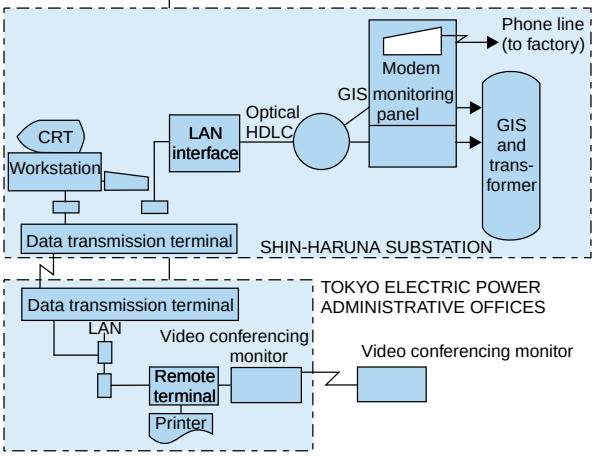

Fig. 1 Monitoring system configuration.

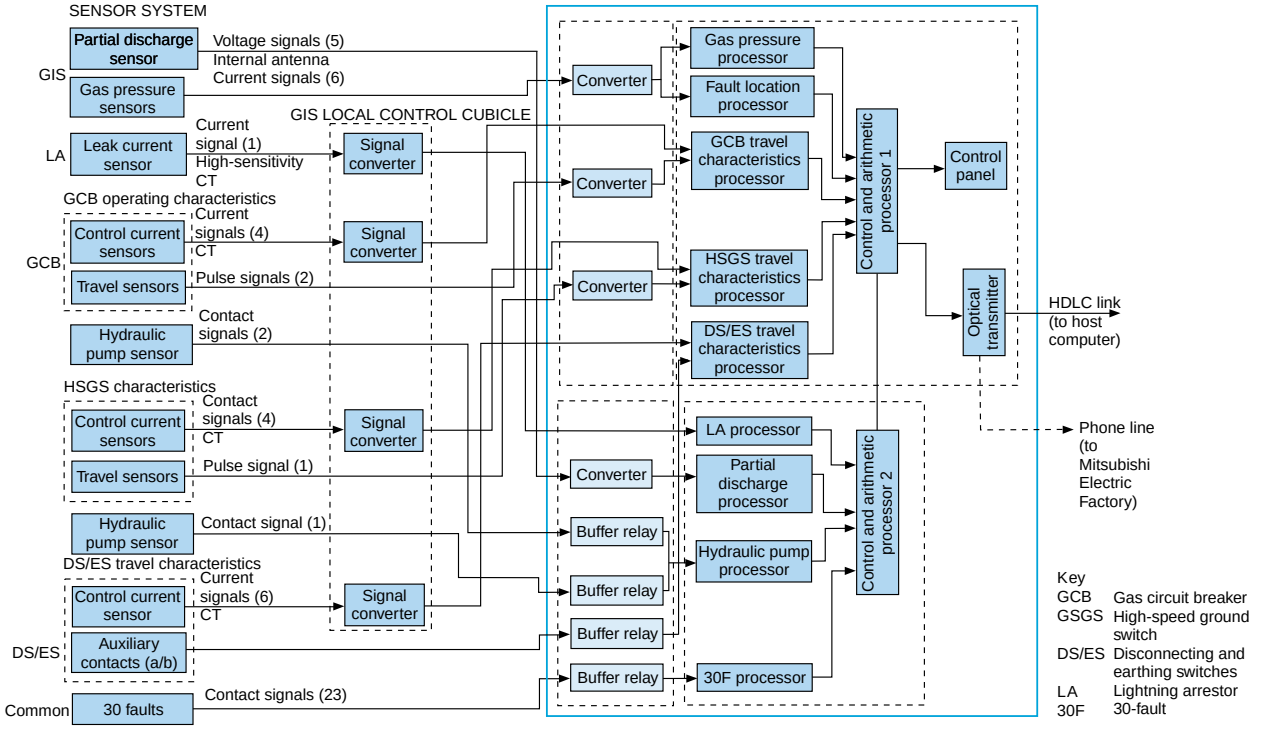

Fig. 2

A Monitoring System for 1,000kV Transformers

Mitsubishi Electric has delivered a transformer monitoring system for use in verification of 1,000kV transformer equipment at the Shin-Haruna UHV Equipment Test Station of Tokyo Electric Power Company. The system consists of sensors and monitoring equipment that analyze the sensor data and provide early warning of abnormal operation.

The monitoring equipment consists of processors for each of the sensor outputs, a control and arithmetic processing unit, an operating panel and an optical-fiber transmitter (Fig. 1). The monitoring equipment can store instrumentation and diagnostic data for up to three months, with display or hardcopy output on demand. The data can be sent to a host computer by the optical-fiber transmitter using the HDLC-NRM protocol, or to the factory by telephone line.

The system monitors the following items.

DISSOLVED GASES. Dissolved gases are extracted from the transformer oil and the concentrations of six gases (CO, H_2, CH_4, C_2H_2, C_2H_4 and C_2H_6) are measured as well as the total combustible gas content. These data are used to provide early warning of local heating, discharge and other abnormalities.

PARTIAL DISCHARGE. A high-frequency current transformer detects partial discharge and acoustic emission (AE) sensors mounted on the wall of the transformer tank detect the associated ultrasonic vibrations. The time delay between the discharge detection (by the current transformer) and ultrasonic detection makes it possible to detect whether the discharge is inside or outside the transformer, and if inside, whether or not it occurred in the transformer tank.

OIL TEMPERATURE. Resistance thermometer bulbs (Pt 100Ω) check the temperatures of the main transformer oil, the load voltage regulator oil and the ambient temperature, and the detected values are compared against specified ranges.

OIL LEVEL MONITORING. Potentiometers on the shaft of conservator-type oil gauges monitor the oil level in the main transformer and load voltage regulator tank. The measured oil levels can be compared against the oil levels predicted on the basis of oil temperature.

ON-LOAD TAP CHANGER OPERATING CHARACTERISTICS. The drive shaft torque during tap changing is measured by a rotary-transformer-type torque sensor. A current sensor measures the current of the motor drive mechanism. Torque and current waveforms are monitored and compared against standard values for each of the six operating modes corresponding to the combination of tap changing command signals and tap positions to verify correct tap changer operation and to resolve the cause of any malfunction that may arise. ❑

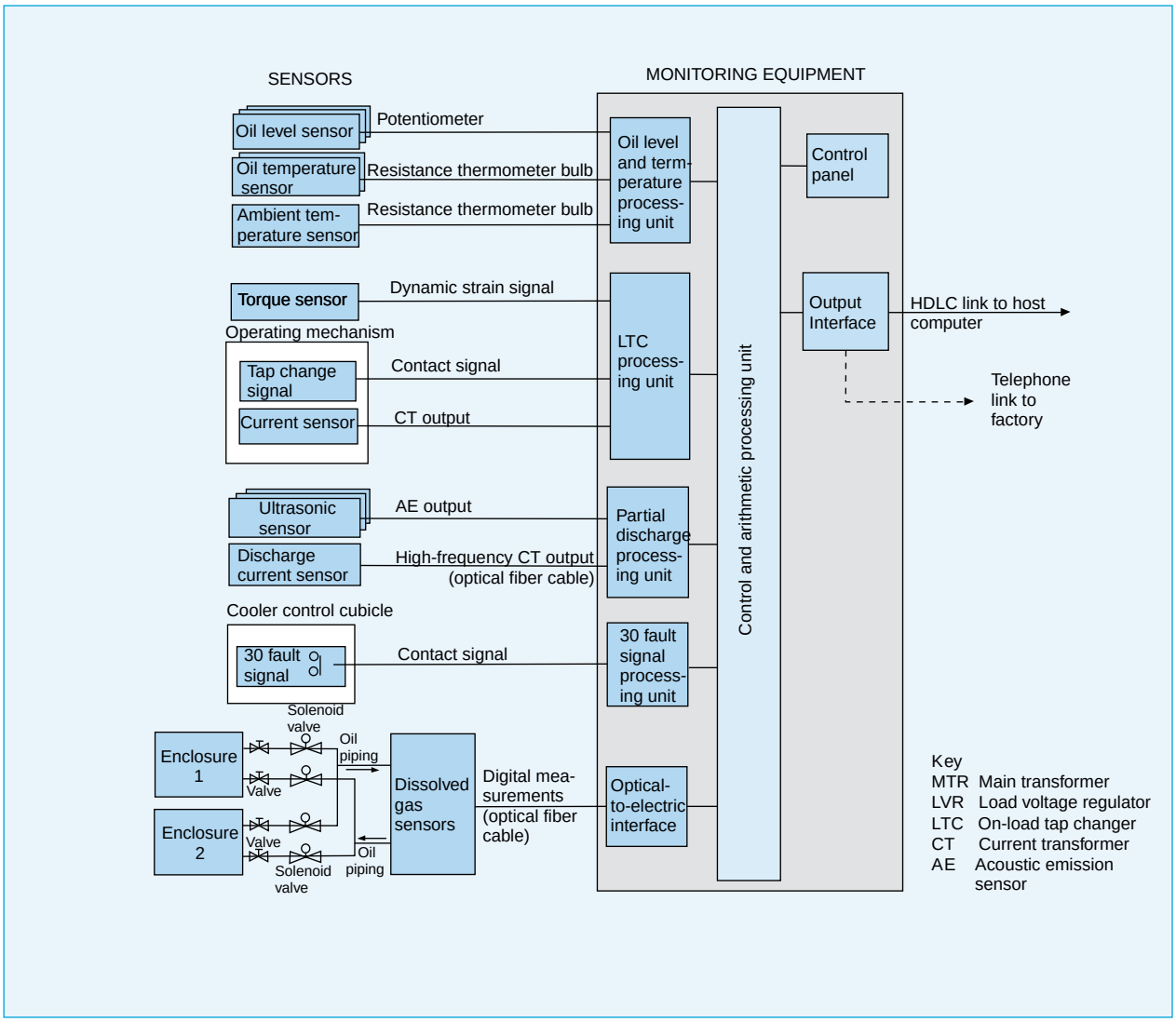

Fig. 1 System block diagram.

MITSUBISHI ELECTRIC OVERSEAS NETWORK (Abridged)

Country	Address		Telephone
U.S.A.	Mitsubishi Electric America, Inc.	5665 Plaza Drive, P.O. Box 6007, Cypress, California 90630-0007	714-220-2500
	Mitsubishi Electronics America, Inc.	5665 Plaza Drive, P.O. Box 6007, Cypress, California 90630-0007	714-220-2500
	Mitsubishi Consumer Electronics America, Inc.	2001 E. Carnegie Avenue, Santa Ana, California 92705	714-261-3200
	Mitsubishi Semiconductor America, Inc.	Three Diamond Lane, Durham, North Carolina 27704	919-479-3333
	Horizon Research, Inc.	1432 Main Street, Waltham, Massachusetts 02154	617-466-8300
	Mitsubishi Electric Power Products Inc.	Thorn Hill Industrial Park, 512 Keystone Drive, Warrendale, Pennsylvania 15086	412-772-2555
	Mitsubishi Electric Manufacturing Cincinnati, Inc.	4773 Bethany Road, Mason, Ohio 45040	513-398-2220
	Astronet Corporation	37 Skyline Drive, Suite 4100, Lake Mary, Florida 32746-6214	407-333-4900
	Powerex, Inc.	Hills Street, Youngwood, Pennsylvania 15697	412-925-7272
	Mitsubishi Electric Research Laboratories, Inc.	201 Broadway, Cambridge, Massachusetts 02139	617-621-7500
Canada	Mitsubishi Electric Sales Canada Inc.	4299 14th Avenue, Markham, Ontario L3R 0J2	905-475-7728
	Mitsubishi Electronics Industries Canada Inc.	1000 Wye Valley Road, Midland, Ontario L4R 4L8	705-526-7871
Mexico	Melco de Mexico S.A. de C.V.	Mariano Escobedo No. 69, Tlalnepantla, Edo. de Mexico	5-565-6269
Brazil	MELCO do Brazil, Com. e Rep. Ltda.	Av. Rio Branco, 123, a 1507, 20040, Rio de Janeiro	21-221-8343
	MELCO-TEC Rep. Com. e Assessoria Tecnica Ltda.	Av. Rio Branco, 123, a 1507, 20040, Rio de Janeiro	21-221-8343
Argentina	MELCO Argentina S.R.L.	Florida 890-20º-Piso, C.P. 1005, Buenos Aires	1-312-6982
Colombia	MELCO de Colombia Ltda.	Calle 35 No. 7-25, Oficinas No. 1201/02, Edificio, Caxdac, Apartado Aereo 29653, Bogotá	1-287-9277
U.K.	Mitsubishi Electric U.K. Ltd.	Travellers Lane, Hatfield, Herts. AL10 8XB, England	1707-276100
	Apricot Computers Ltd.	3500 Parkside, Birmingham Business Park, Birmingham, B37 7YS, England	21-717-7171
	Mitsubishi Electric Europe Coordination Center	Centre Point (18th Floor), 103 New Oxford Street, London, WC1A 1EB	71-379-7160
France	Mitsubishi Electric France S.A.	55, Avenue de Colmar, 92563, Rueil Malmaison Cedex	1-47-08-78-00
Netherlands	Mitsubishi Electric Netherlands B.V.	3rd Floor, Parnassustoren, Locatellikade 1, 1076 AZ, Amsterdam	20-6790094
Germany	Mitsubishi Electric Europe GmbH	Gothaer Strasse 8, 40880 Ratingen	2102-4860
	Mitsubishi Semiconductor Europe GmbH	Konrad Zuse Strasse 1, 52477 Alsdorf	2404-990
Spain	MELCO Iberica S.A. Barcelona Office	Polígono Industrial "Can Magi", Calle Joan Buscallà 2-4, Apartado de Correos 420, 08190 Sant Cugat del Vallés, Barcelona	3-589-3900
Italy	Mitsubishi Electric Europe GmbH, Milano Office	Centro Direzionale Colleoni, Palazzo Perseo-Ingresso 2, Via Paracelso 12, 20041 Agrate Brianza, Milano	39-60531
China	Shanghai Mitsubishi Elevator Co., Ltd.	811 Jiang Chuan Rd., Minhang, Shanghai	21-4303030
Hong Kong	Mitsubishi Electric (H.K.) Ltd.	41st Floor, Manulife Tower, 169 Electric Road, North Point	510-0555
	Ryoden Holdings Ltd.	10th Floor, Manulife Tower, 169 Electric Road, North Point	887-8870
	Ryoden Merchandising Co., Ltd.	32nd Floor, Manulife Tower, 169 Electric Road, North Point	510-0777
Korea	KEFICO Corporation	410, Dangjung-Dong, Kunpo, Kyunggi-Do	343-51-1403
Taiwan	MELCO Taiwan Co., Ltd.	2nd Floor, Chung-Ling Bldg., No. 363, Sec. 2, Fu-Hsing S. Road, Taipei	2-733-2383
	Shihlin Electric & Engineering Corp.	No. 75, Sec. 6, Chung Shan N. Rd., Taipei	2-834-2662
	China Ryoden Co., Ltd.	Chung-Ling Bldg., No. 363, Sec. 2, Fu-Hsing S. Road, Taipei	2-733-3424
Singapore	Mitsubishi Electric Singapore Pte. Ltd.	152 Beach Road #11-06/08, Gateway East, Singapore 189721	295-5055
	Mitsubishi Electric Sales Singapore Pte. Ltd.	307 Alexandra Road #05-01/02, Mitsubishi Electric Building, Singapore 159943	473-2308
	Mitsubishi Electronics Manufacturing Singapore Pte. Ltd.	3000, Marsiling Road, Singapore 739108	269-9711
	Mitsubishi Electric Asia Coordination Center	307 Alexandra Road #02-02, Mitsubishi Electric Building, Singapore 159943	479-9100
Malaysia	Mitsubishi Electric (Malaysia) Sdn. Bhd.	Plo 32, Kawasan Perindustrian Senai, 81400 Senai, Johor	7-5996060
	Antah MELCO Sales & Services Sdn. Bhd.	3 Jalan 13/1, 46860 Petaling Jaya, Selangor, P.O. Box 1036	3-756-8322
	Ryoden (Malaysia) Sdn. Bhd.	2nd Fl., Wisma Yan, Nos. 17 & 19, Jalan Selangor, 46050 Petaling Jaya	3-755-3277
Thailand	Kang Yong Watana Co., Ltd.	15th Floor, Vanit Bldg., 1126/1, New Petchburi Road, Phayathai, Bangkok 10400	2-255-8550
	Kang Yong Electric Co., Ltd.	67 Moo 11, Bangna-Trad Highway, Km. 20 Bang Plee, Samutprakarn 10540	2-312-8151
	MELCO Manufacturing (Thailand) Co., Ltd.	86 Moo 4, Km. 23 Bangna-Trad, Bangplee, Semudparkarn 10540	2-312-8350~3
	Mitsubishi Elevator Asia Co., Ltd.	Bangpakong Industrial Estate, 700/86~92, Moo 6 Tambon Don Hua Roh, Muang District Chonburi 20000	38-213-170
	Mitsubishi Electric Asia Coordination Center (Thailand)	17th Floor, Bangna Tower, 2/3 Moo 14, Bangna-Trad Highway 6.5 Km, Bangkawe, Bang Plee, Samutprakarn 10540	2-312-0155~7
Philippines	International Elevator & Equipment, Inc.	Km. 23 West Service Road, South Superhighway, Cupang, Muntinlupa, Metro Manila	2-842-3161~5
Australia	Mitsubishi Electric Australia Pty. Ltd.	348 Victoria Road, Postal Bag No. 2, Rydalmere, N.S.W. 2116	2-684-7200
New Zealand	MELCO Sales (N.Z.) Ltd.	1 Parliament St., Lower Hutt, P.O. Box 30-772 Wellington	4-569-7350
Representatives			
China	Mitsubishi Electric Corp. Beijing Office	SCITE Tower, Rm. 1609, Jianguo Menwai, Dajie 22, Beijing	1-512-3222
	Mitsubishi Electric Corp. Shanghai Office	Room No. 1506-8, Shanghai Union Building 100, Yanan-East Street, Shanghai	21-320-2010
Korea	Mitsubishi Electric Corp. Seoul Office	Daehan Kyoyuk Insurance Bldg., Room No. 1204 #1, Chongno 1-ka, Chongno-ku, Seoul	2-732-1531~2
Viet Nam	Mitsubishi Electric Corp. Ho Chi Minh City Office	8 B2, Han Nam Officetel 65, Nguyen Du St., 1st District, Ho Chi Minh City	8-243-984

MITSUBISHI ELECTRIC CORPORATION
HEAD OFFICE: MITSUBISHI DENKI BLDG., MARUNOUCHI, TOKYO 100-8310, FAX 03-3218-3455